plasma

MDPI

Review

Formation of Fine Structures in Incompressible Hall Magnetohydrodynamic Turbulence Simulations

Hideaki Miura

National Institute for Fusion Science, 322-6 Oroshi, Toki 509-5292, Gifu, Japan; miura.hideaki@nifs.ac.jp

Abstract: Hall magnetohydrodynamic simulations are often carried out to study the subjects of instabilities and turbulence of space and nuclear fusion plasmas in which sub-ion-scale effects are important. Hall effects on a structure formation at a small scale in homogeneous and isotropic turbulence are reviewed together with a simple comparison to a (non-Hall) MHD turbulence simulation. A comparison between MHD and Hall MHD simulations highlights a fine structure in Hall MHD turbulence. This enhancement of the fine structures by the Hall term can be understood in relation to the whistler waves at the sub-ion scale. The generation and enhancement of fine-scale sheet, filamentary, or tubular structures do not necessarily contradict one another.

Keywords: Hall MHD; coherent structures; sheet; filament

1. Introduction

Hall magnetohydrodynamic (MHD) equations are variants of MHD equations and can be derived from either Braginskii's two-fluid model or the Vlasov–Boltzmann equation, neglecting electron inertia, finite ion Larmor radius effects, and other fine-scale effects [1].

The Hall term appears in the generalized Ohmic law to represent the effects of finite ion-skin-depth or ion-inertia-scale. Hereafter, we refer to a scale shorter than the ion-skin-depth as the sub-ion scale. The introduction of the Hall term changes the frozen-in condition, conservation laws, inviscid invariants (energy, magnetic helicity, and hybrid helicity), the linear dispersion relation of waves, and consequent plasma dynamics, including dynamos and magnetic reconnection. This modification has encouraged many studies, from Alfvén waves, whistle waves, and double-Beltrami flows to more fundamental and mathematical subjects [2–21]. These changes enrich the physics related to the sub-ion scale.

The Hall MHD model is widely used to study various subjects such as the Kelvin–Helmholtz instability, Rayleigh–Taylor, and some other instabilities, sometimes together with finite Larmor radius effects (gyro-viscosity) [22–38].

The Hall term also changes various aspects of turbulence, including dynamo action [39–43] and magnetic reconnection [44–46].

The applicability of the Hall MHD model to plasma dynamics has been also investigated [47–50]. Schnack et al. [48] have shown that Hall MHD can be derived for studying plasma physics in the inner heliosphere, shock tubes, and other subjects. In Ref. [49], it is shown that the Hall MHD model can be a reliable one for studying the ion temperature gradient instability for a certain scale range. Papini et al. [50] carried out turbulence simulations of both Hall MHD and Hall MHD-PIC hybrid simulations. They concluded that the Hall MHD model, to a large extent, captures the scale from the MHD scale to the sub-ion scale.

There are also many studies of Hall MHD turbulence. See Refs. [47,51–56] and references therein for an overview of Hall MHD turbulence with a wide scope. Hereafter, we simply focus on a small category of numerical simulations of turbulence often called homogeneous and isotropic incompressible Hall MHD turbulence, mainly in the context of fine structure formation. Studies on other subjects are mentioned briefly.

check for updates

Citation: Miura, H. Formation of Fine Structures in Incompressible Hall Magnetohydrodynamic Turbulence Simulations. *Plasma* **2024**, *7*, 793–815. https://doi.org/10.3390/plasma7040042

Academic Editors: Eun-jin Kim and Andrey Starikovskiy

Received: 25 June 2024
Revised: 18 July 2024
Accepted: 3 October 2024
Published: 11 October 2024

This paper is organized as follows. In Section 2, numerical simulations of Hall MHD turbulence are introduced. In Section 3, topics of the energy spectra of Hall MHD turbulence are reviewed briefly. In Section 4, formation of coherent or fine structures in incompressible Hall MHD turbulence is presented, together with a comparison to (non-Hall) MHD turbulence. Section 5 presents a summary.

2. Numerical Simulations of Hall MHD Turbulence

Incompressible Hall MHD equations can be described as follows:

$$\frac{\partial u_i}{\partial t} = -\frac{\partial}{\partial x_j}(u_i u_j) - \frac{\partial p}{\partial x_i} + \epsilon_{ijk} J_j B_k + \nu \frac{\partial^2 u_j}{\partial x_j \partial x_j} + f_i^u, \tag{1}$$

$$\frac{\partial B_i}{\partial t} = -\epsilon_{ijk} \frac{\partial}{\partial x_j}[-\epsilon_{klm}(u_l - \epsilon_H J_l) B_m + \eta J_k] + f_i^b, \tag{2}$$

$$\frac{\partial u_i}{\partial x_i} = 0, \tag{3}$$

$$\frac{\partial B_i}{\partial x_i} = 0. \tag{4}$$

The symbols B_i, $J_i = \epsilon_{ijk}\partial_j B_k$, and u_i represent the i-th components of the magnetic field, current density, and velocity field vectors, respectively. The symbol ϵ_{ijk} is Levi-Civita's anti-symmetric tensor. Equations (1)–(4) are already normalized by some representative variables. See Refs. [57,58] for the normalization. The Hall parameter ϵ_H represents the ratio of the ion-skin-depth to the system size.

In Equations (1)–(4), the Ohmic law $E_k = -\epsilon_{klm} u_l B_m + \eta J_k$ in resistive MHD equations has been replaced by the generalized Ohmic law $E_k = -\epsilon_{klm} u_l^e B_m + \eta J_k$, where E_k is the k-th component of the electric field, and $u_k^e = u_k - \epsilon_H J_k$ is the electron velocity.

Among the various differences between the Hall MHD model and the MHD one, the emergence of whistler waves that propagate along magnetic field lines with a high frequency of

$$\omega^2 = \left(\frac{V_A^2}{\Omega}\right)^2 k^2 k_\parallel^2 \tag{5}$$

is a key feature of a Hall MHD simulation, where $k_\parallel$, V_A, Ω, and ω are the wave vector parallel to the background magnetic field, Alfvén velocity, ion cyclotron frequency, and frequency, respectively [48].

The appearance of whistler waves brings about not only an excitation of high wave-number Fourier coefficients of the magnetic field but also a severe restriction in the time-step width to satisfy the stability condition of the dispersive wave. Furthermore, we need to sufficiently resolve the nonlinear transport of the magnetic field energy from low-wave-number to high-wave-number Fourier coefficients. One needs a high resolution (many grid points in real space) to resolve both the MHD scale and sub-ion scale and an extremely small time-step width in a Hall MHD turbulence simulation to satisfy the requirements.

In order to overcome the severe requirements and to elucidate the physics of turbulence by simulations, we often use hyper-diffusivity, which is added to the right-hand side of Equations (1) and (2). We also use this classic technique in this article. However, we can also consider carrying out a large eddy simulation (LES) instead of the hyper-diffusivity. Although we do not use numerical data from an LES in this article, it is worth considering carrying out an LES to overcome the severe numerical restrictions. See Appendix A for an outline of our LES.

3. Energy Spectra and Related Topics in Hall MHD Turbulence

There are many theoretical and numerical studies on MHD and Hall MHD turbulence. With respect to the theoretical aspects of MHD turbulence, especially in relation to hydrodynamic turbulence, see textbooks [59–61].

Among various subjects of turbulence studies, scaling laws in energy spectra are of central interest. Space satellite measurements report scaling laws of the frequency f by $f^{-1.7}$ in the MHD-scale (the scale larger than ion-skin-depth) and $f^{-2.6}$ in the sub-ion scale (the scale smaller than the ion-skin-depth) of solar winds and coronal plasma [62,63]. Recent advancements in Parker Solar Probe (PSP) measurements provide further information. Since a study using POP data exceeds the scope of this article, see reviews and articles such as Refs. [64–68].

The existence of scaling regimes are closely related to the classic phenomenology of MHD turbulence, such as Kolmogorov's theory, which predicts $E_M(k) \sim k^{-5/3}$, and the Iroshnikov–Kraichnan theory, which predicts $E_M(k) \sim k^{-3/2}$ at the MHD scale, where $E_M(k)$ is the magnetic energy spectrum, while the kinetic energy spectrum is represented by $E_K(k)$ (see Refs. [60,61] for these topics). The phenomenology of turbulence under a guiding magnetic field is given by Goldreich and Sridhar as $E_M(k_\perp) \sim k_\perp^\alpha$ [69]. Succeeding theories and simulations support basic views given by Goldreich and Sridhar, which are typically seen in the decomposition of the wave-number vector to parallel ($k_\parallel$) and perpendicular ($k_\perp$) components [70–76]. Nevertheless, in the context of homogeneous and isotropic turbulence, we consider Kolmogorov's or Iroshnikov-Kraichnan's phenomenology rather than these more recent theories because of the absence of the guiding magnetic field.

As in the MHD scale, a scaling law in the sub-ion scale is also studied extensively. An incompressible Hall MHD turbulence simulation is often expected to show $E_M(k) \propto k^{-7/3}$. Numerical simulations of Hall MHD turbulence support the $k^{-7/3}$ law at the sub-ion scale, whether the simulation is a shell model [77,78] or a three-dimensional numerical simulation [42,57,58,79–82].

Although the scaling law $E_M(k) \propto k^{-7/3}$ has been widely accepted, another scaling law in the sub-ion scale of the magnetic energy spectrum $E_M(k) \sim k^{-8/3}$ has been reported by Meyrand and Galtier for electron MHD turbulence [83]. Below we see that an incompressible Hall MHD simulation can show the scaling law of $E_M(k) \sim k^{-8/3}$ as well.

In Figure 1, $E_K(k)$ and $E_M(k)$ are obtained in a forced Hall MHD turbulence simulation, with the magnetic Prandtl number $Pr_M = \nu/\eta = 100$ plotted together with compensated energy spectra. The external force is given to the equation of motion with a fixed amplitude at $k \leq 3$ with random Fourier phases. The amplitude of the external force is predetermined at a level at which the force does not cause an excessive raise of the tail of the energy spectrum. The abscissa is normalized by the ion-skin-depth so that the region $\epsilon_H k > 1$ represents the sub-ion scale. This computation is similar to those presented in Ref. [84] by the pseudo-spectral method and the Runge–Kutta–Gill scheme. We use either the FFTE [85], P3DFFT [86], or FT3D [87] three-dimensional libraries, depending on the supercomputer. A hyper-diffusivity is also used to suppress a very high-k region. (Another scaling of $E_M(k) \sim k^{-5/2}$ has been reported in Ref. [84], without using hyper-diffusivity.) At the sub-ion scale, $E_K(k) \propto k^{-17/3}$, while $E_M(k) \propto k^{-8/3}$ rather than the well-known $E_M(k) \propto k^{-7/3}$ scaling law. As we see later, coherent structures in MHD and Hall MHD turbulence are often considerably influenced by the magnetic Prandtl number Pr_M. We need to clarify a detailed setup of a numerical simulation in order to compare our numerical results to an observational result and choose an appropriate Pr_M.

While scaling laws in the energy spectrum have been studied extensively, those in the real-space structure functions (von Kármán–Howarth-like scaling laws, or a so-called exact relation of correlation functions), intermittency, and extended self-similarity are closely related to the scaling laws in the energy spectrum. With respect to the structure functions of MHD turbulence, a formulation given by Politano and Pouquet [88,89] for the third-order structure function (von Kármán–Howarth equation) and succeeding works provides an important foundation [90–102].

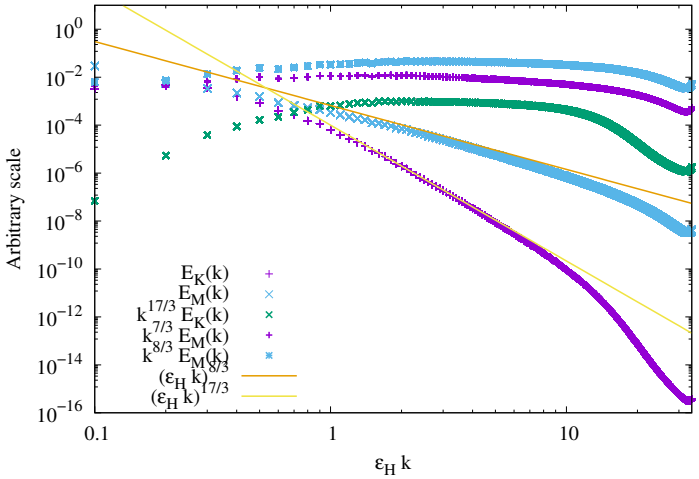

Figure 1. The kinetic and magnetic energy spectrum $E_K(k)$, with $E_M(k)$ obtained in a forced Hall MHD turbulence simulation with $Pr_M = 100$ and $N^3 = 1024^3$ grid points. Their compensated energy spectra are also plotted.

There are other important keywords for Hall MHD turbulence. Anisotropy, (inverse) cascade, dissipation, and energy transfer are the typical important keywords of both MHD turbulence and Hall MHD turbulence. We do not review these subjects and move on to the formation of fine structures. See earlier studies [41–43,82,103–113] for these subjects.

There are also interesting subjects such as a closure theory, as in Ref. [114], which should be studied further.

4. Formation of Coherent Structures

4.1. Discussions of Coherent Structures in MHD Turbulence

Formation of coherent structures has been one of important subjects of MHD turbulence. Recent studies discuss the emergence of coherent structures more closely, sometimes reporting not only current sheets but also filaments of currents and/or vortices [115–118].

From a point of view of numerical simulations, the emergence of coherent structures is closely related to energy dissipation, energy transfer, intermittency, and other phenomena. In the context of structure formation, a coherent structure can mean not only a large-scale structure but also a fine, small-scale one. In this article, we include both of these meanings in the expression coherent structures. See also textbook [59], reviews [119–124], and articles [46,104,117,125–131] for coherent structures in (non-Hall) MHD turbulence.

Greco et al.[127] have discussed a relation between the Probability Density Function (PDF) of the current density and the coherent structures of the current density. In Figure 2, Figure 3 of Ref. [127] was reprinted with permission from Greco et al., Astrophysical Journal 691:L111-L114 (2009). Copyright (2009) by the Institute of Physics. In the figure, PDF of the current density from the 2D simulation in Ref. [127], and magnetic field lines (contours of constant magnetic potential) corresponding to the regions I-III of the PDF. The PDF of the current density has a skewed profile with a tail much wider than the Gaussian, showing a clear tendency of spatial intermittency. It shows a relation between the parts of the PDF (the head, body, and tail) and magnetic field lines. This work reveals a contribution of coherent structures to the statistics of the current and thus to the intermittency of turbulence.

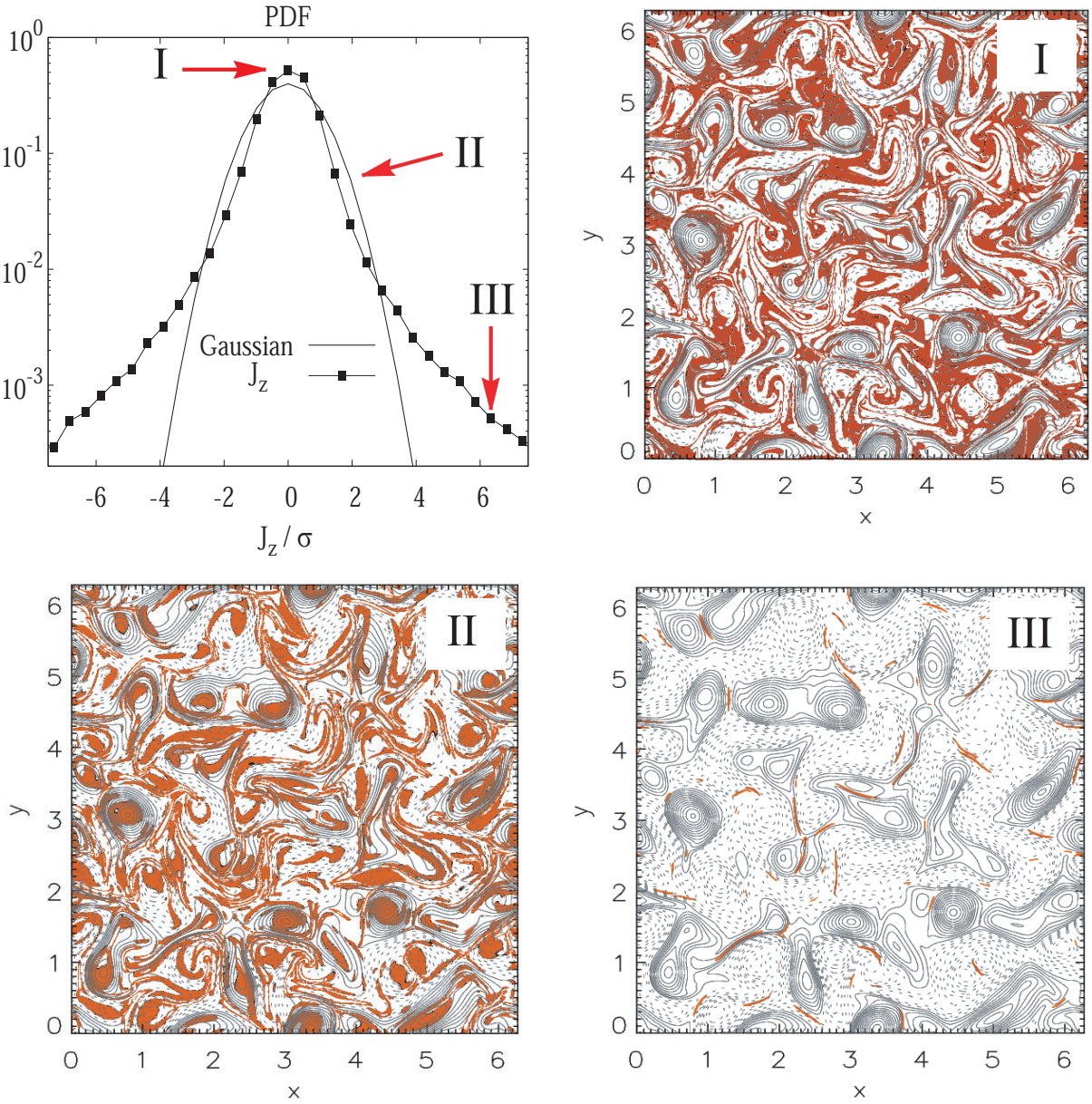

Figure 2. PDF of the current density and magnetic field lines (contours of constant magnetic potential) corresponding to the regions I–III of the PDF. Figure reprinted with permission from Greco et al., Astrophysical Journal 691:L111–L114 (2009) [127], 1 February 2009, doi:10.1088/0004-637X/691/2/L111 [127]. Copyright (2009) by the Institute of Physics.

Sahoo et al. have carried out numerical simulations of both freely decaying and forced turbulence over a range of Pr_M [118]. In that work, the isosurfaces of the current density, vorticity, and energy dissipation are presented. A high-Pr_M simulation tends to give fine structures of the current density and vorticity, while the large-scale structures are found in the isosurfaces of the magnetic energy dissipation of a high-Pr_M simulation. In Figure 3, isosurfaces of the current density of MHD turbulence with various magnetic Prandtl numbers with or without external forcing, presented in Ref. [118] as Figure 27, are reproduced with permission by the authors and the Institute of Physics. These views are presented in the literature together with PDFs of the velocity and magnetic field increments, the plots of the velocity and magnetic field vector gradient invariants, and some other important statistical information.

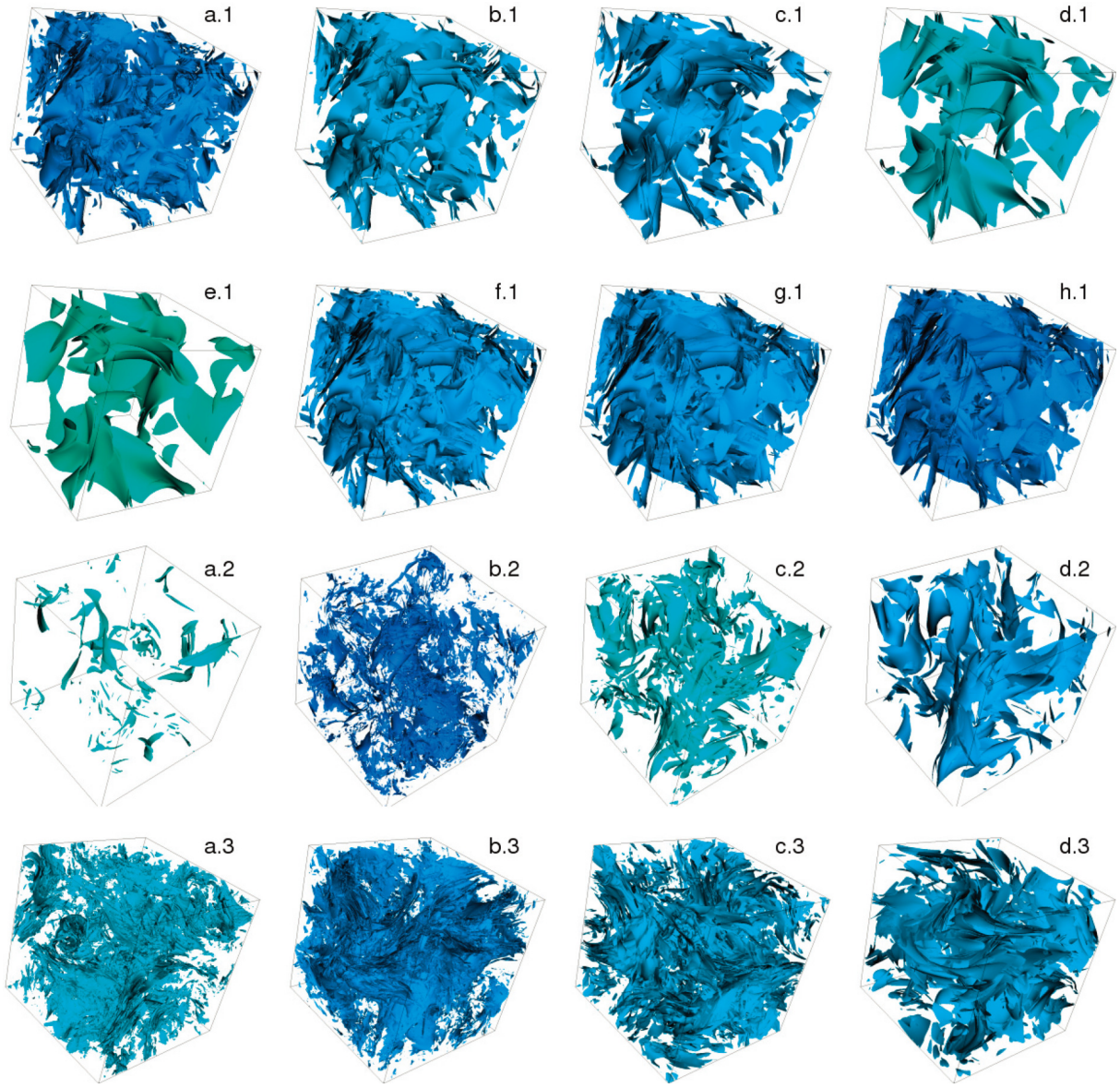

Figure 3. Isosurfaces of the current density of MHD turbulence with various magnetic Prandtl numbers with and without external forcing. The panels (**a.1**)–(**d.3**) is for different magnetic Prandtl numbers from $Pr_M = 0.1$ to 10.0 and other numerical conditions. Magnetic Prandtl numbers are (**a.1**) $PrM = 0.1$, (**b.1**) $PrM = 0.5$, (**c.1**) $PrM = 1.0$, (**d.1**) $PrM = 5.0$, (**e.1**) $PrM = 10.0$, (**f.1**) $PrM = 1.0$, (**g.1**) $PrM = 5.0$, (**h.1**) $PrM = 10.0$, (**a.2**) $PrM = 0.01$, (**b.2**) $PrM = 0.1$, (**c.2**) $PrM = 1.0$, (**d.2**) $PrM = 10.0$, (**a.3**) $PrM = 0.01$, (**b.3**) $PrM = 0.1$, (**c.3**) $PrM = 1.0$, (**d.3**) $PrM = 10.0$, respectively. The panels (**a.1**)–(**d.2**) are for decaying simulations while (**a.3**)–(**d.3**) are for forced turbulence. See Table 1 of [118] for detailed numerical conditions. Figure reprinted with permission from Sahoo et al.[118]. © IOP Publishing Ltd and Deutsche Physikalische Gesellschaft. Reproduced by permission of IOP Publishing. https://doi.org/10.1088/1367-2630/13/1/013036, CC BY-NC-SA https://creativecommons.org/licenses/by-nc-sa/3.0/ (accessed on 25 June 2024).

Zhdankin et al. have highlighted statistics of the current sheets [129] as well as the typical role of coherent turbulence structures in the energy dissipation [130]. They present numerical procedures to identify the current sheets in Ref. [129] and study the orbit of magnetic field lines on the current sheets. In Ref. [130], they studied energy dissipation in MHD turbulence and related the study to coherent structures. They report that the main part of the energy dissipation occurs in large-scale coherent structures (current sheets), while the dissipation spreads over a wide range of the wave-number from the inertial

range to the dissipation range and exhibits coherent structures (current sheets) and small reconnection events (nanoflares).

While the current sheets are recognized as the center of interest in various subjects related to MHD turbulence, rolls of vortices and currents due to a local Kelvin–Helmholtz instability in turbulence have been reported [126]. In Figure 4, the roll-up of a current sheet in an MHD turbulence simulation is presented. This figure, a reproduction of Figure 2 from [126] used with permission, clearly captures a fine-scale roll of current in a high-resolution MHD turbulence simulation. We also note that, in a different regime of physical parameters (numerical settings of simulations), vortex tubes can be more dominant. For example, Kitiashvili et al. [132], Kivotides [133], and Silva et al. [134] report vortex tubes in solar convection.

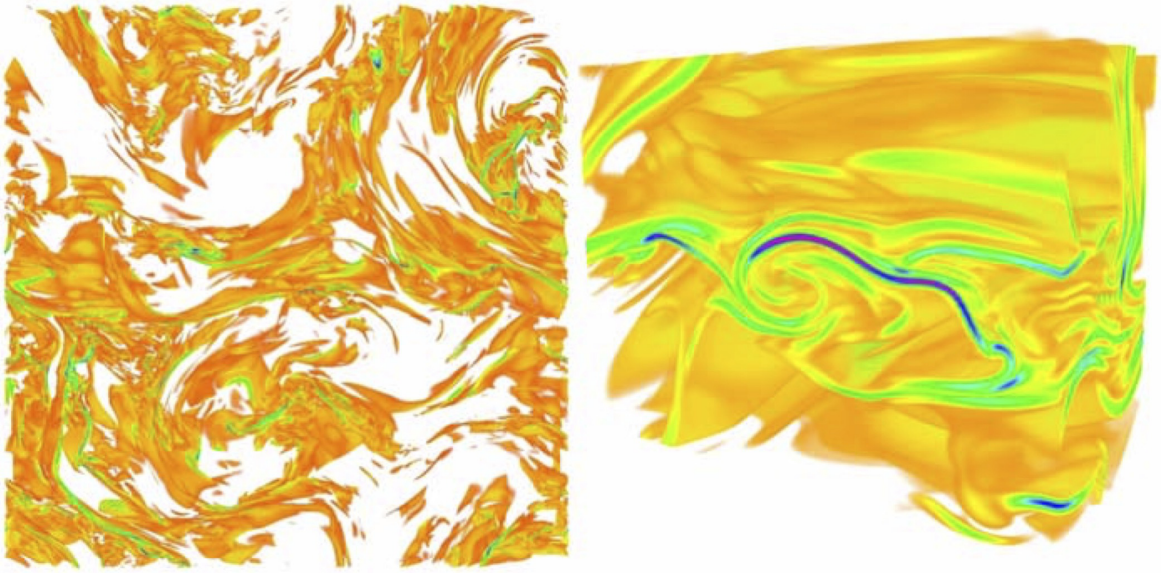

Figure 4. Figure 2 from [126], in which current densities in the full box (**left**) and in a subregion (**right**) of a simulation showing folding and rolling of the current sheets are presented. Figure reprinted with permission from the authors and American Physical Society. Copyright (2009) by the American Physical Society.

4.2. Fine Structures in Hall MHD Turbulence

Coherent or fine structures in Hall MHD turbulence are often studied as an extension of numerical studies of (non-Hall) MHD turbulence. As Marino and Sorriso-Valvo [56] have reviewed recently, a role of the Hall term in coherent structures is a focus of discussion. While many works support the formation of a large-scale magnetic structure (or a large current sheet), some works present formation of a fine structure such as current and vortex filaments. A large-scale magnetic structure or a large current sheet is considered to explain a large jump in magnetic field signals reported by spacecraft observations. As we have seen in the work of Zhdankin et al. [130], a current sheet involves a wide range of scale from the largest scale of the inertial range to the dissipation scale. However, simultaneously, we often observe fine structures as well. Formation of fine structures does not necessarily contradict the formation of a large-scale structure.

To the best knowledge of the authors, formation of coherent or fine structures is often different between a freely decaying simulation and a forced simulation, whether it is Hall MHD turbulence or (non-Hall) MHD turbulence. Various aspects of a freely decaying turbulence simulation depend on details of the initial condition. The ratio of the kinetic and magnetic energies and the three inviscid invariants, including influences of helicity [55,135,136] in particular, are considered crucial roles there. Although it is difficult to assert the nature of coherent or fine structures in a freely decaying turbulence because of

this initial condition dependence, freely decaying turbulence simulations are carried out partially because a decay law in turbulence stimulates wide interest (whether it is MHD or Hall MHD) [60]. On the other hand, a forced turbulence simulation is influenced by the nature of an external force. The formation can be also different between turbulence with and without magnetization.

4.2.1. Decaying Homogeneous and Isotropic Turbulence

An advantage of studying freely decaying turbulence is that a comparison between MHD and Hall MHD turbulence is clear. By giving the same initial condition, ν, η, and the time-step width, we can attribute any single difference to the Hall effect, although we need to take care with the difference in numerical resolution required by the two kinds of simulations.

In Figure 5, isosurfaces of the enstrophy density (green) $E_\omega = \langle \omega_i \omega_i \rangle / 2$ and the current density (gray) $J = \langle J_i J_i \rangle / 2$ in decaying isotropic simulations of (a) MHD ($\epsilon_H = 0$) and (b) Hall MHD ($\epsilon_H = 0.05$) turbulence are shown, where $\omega_i = \epsilon_{ijk} \partial_j u_k$ and $J_i = \epsilon_{ijk} \partial_j B_k$ are the i-th component of the vorticity and the current density, respectively. These two numerical simulations start from the same initial condition with the same kinetic and magnetic energies as those in Refs. [57,58] and are carried out with $\nu = \eta = 5 \times 10^{-5}$ and $N^3 = 2048^3$ grid points. The thresholds of E_ω and J are given by four times the deviation above the mean value of each quantity, respectively.

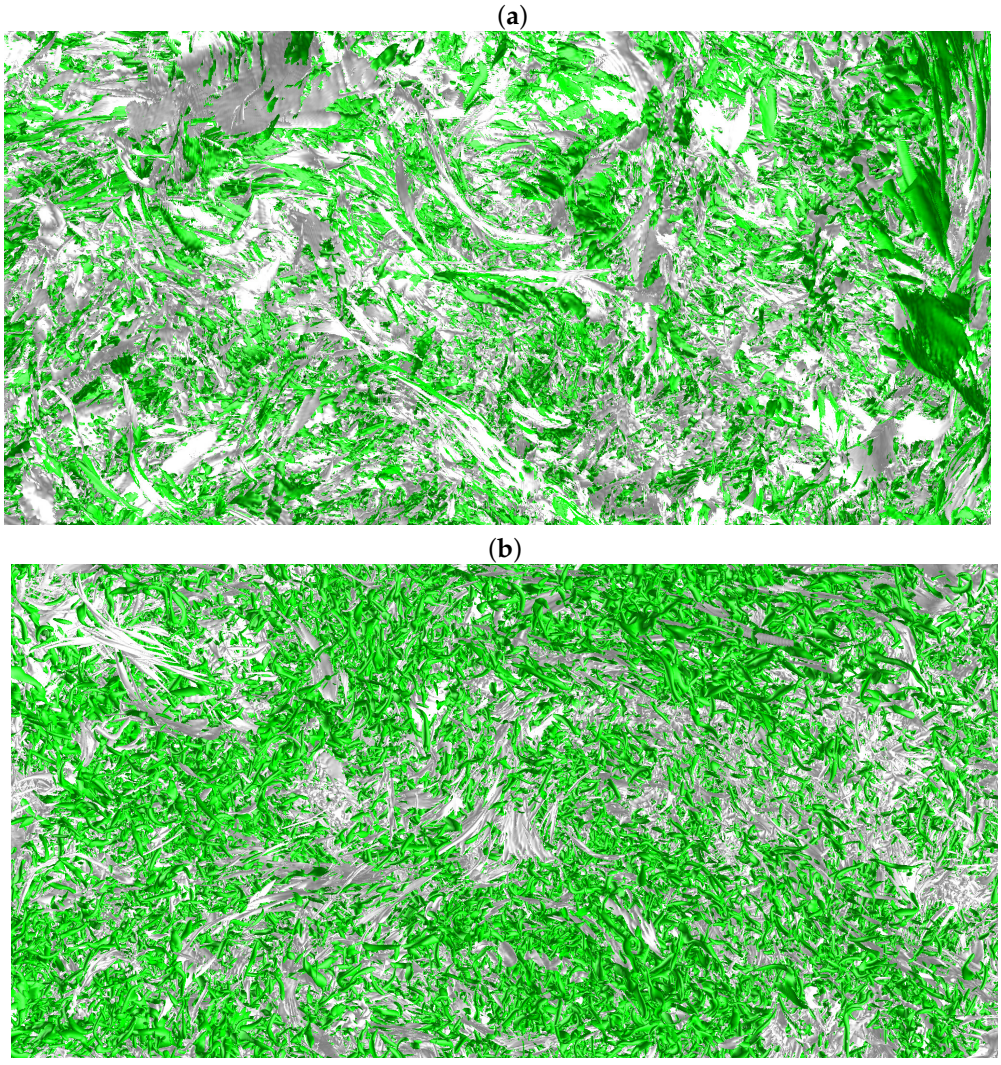

Figure 5. Isosurfaces of the enstrophy density (green) and the current density (gray) in freely-decaying (**a**) MHD and (**b**) Hall MHD ($\epsilon_H = 0.05$) simulations. Simulation data were visualized by VISMO [137].

In Figure 5a, both green and gray isosurfaces are thin and fine sheets or threads. In comparison to simulations with a lower resolution (and thus larger ν and η) reported in earlier works [57,58], the current sheets are smaller and narrower. This suggests that the large-scale current sheets observed in MHD turbulence in Refs. [57,58] can be either unstable or covered by fine-scale structures (signals of high wave-number components), in a higher Lundquist number simulation.

In Figure 5b, the gray isosurfaces of J are either fine threads or fine filaments, while the green isosurfaces of E_ω are tubular or filamentary. These structures are much finer than those in Figure 5a, taking the shape of a tube (green) or a very fine filament (gray). As has been noted already, since both the MHD and Hall MHD simulations start from the same initial condition and the same diffusive coefficients, all differences between the two simulations are finally attributed to the Hall effect.

Based on these simulations, the Hall term is considered to enhance the filamentary or tubular structures of J and E_ω, which represent the excitation of the small scale of the magnetic and velocity fields. A similar result regarding structure formation in comparison between freely decaying MHD and Hall MHD turbulence has been given for another initial condition, in which the kinetic and magnetic energy are the same but have different decaying properties [81]. Our current understanding is that the Hall term allows for the roll-up of a vortex sheet to a vortex tube through the change of the frozen-in condition, and then a current filament is formed through either an entrainment of a current sheet by a vortex tube or an excitation of whistler waves.

We note that Stawarz and Pouquet have also carried out freely decaying Hall MHD turbulence simulations [138]. They report that the Hall term makes the current sheets thinner, while the width of the vorticity makes them wider, although they are non-committal on the detail of vortex strictures in the work. They do not report formation of fine structures. We need further study to clarify what is a key difference between the simulations in Figure 5 and the results in Ref. [138].

An influence of the enhancement of a filamentary or tubular structure can reach a scale larger than the ion-skin-depth $1/\epsilon_H$. In Ref. [58], it is shown that changes to the structures are observed even at the MHD scale. This indicates that the Hall effect, which changes only the physics in the sub-ion scale, can reach the MHD scale. Banerjee and Halder have studied the range of nonlinear interactions in Hall MHD turbulence recently [139]. Studying how far the Hall term can reach at a scale larger than the ion-skin-depth and how the Hall term can influence the large scale may be an interesting subject.

4.2.2. Forced Homogeneous and Isotropic Turbulence

Next, we see an example of structure formation in forced isotropic simulations.

In a numerical simulation of MHD and Hall MHD turbulence, formation of the current sheets or large-scale magnetic field structures with a large jump are often reported. However, the emergence of the coherent structure can depend on the magnetic Prandtl number $Pr_M = \nu/\eta$, as Sahoo et al. [118] have reported for MHD turbulence. In Figure 6, Figure 4 in Ref. [84] is presented (reused in accordance with the American Physical Society's copyright policy). Isosurfaces of E_ω (green) and J (gray) in (a) forced Hall MHD turbulence of $Pr_M = 10$ ($\epsilon_H = 0.20, \nu = 1 \times 10^{-3}, \eta = 1 \times 10^{-4}$), (b) forced Hall MHD turbulence of $Pr_M = 100$ ($\epsilon_H = 0.20, \nu = 1 \times 10^{-2}, \eta = 1 \times 10^{-4}$), and (c) forced MHD turbulence of $Pr_M = 100$ ($\epsilon_H = 0, \nu = 1 \times 10^{-2}, \eta = 1 \times 10^{-4}$). One finds that J-isosurfaces in Figure 6a,b are filamentary, while those in Figure 6c are flattened. In this sense, the Hall term appears to enhance filamentary structures. This indicates that we need to pay attention to the value of Pr_M (or a corresponding concept in a kinetic simulation) if we study coherent structure formation of a phenomena in which Pr_M is supposed to be large, as we have seen in freely decaying simulations.

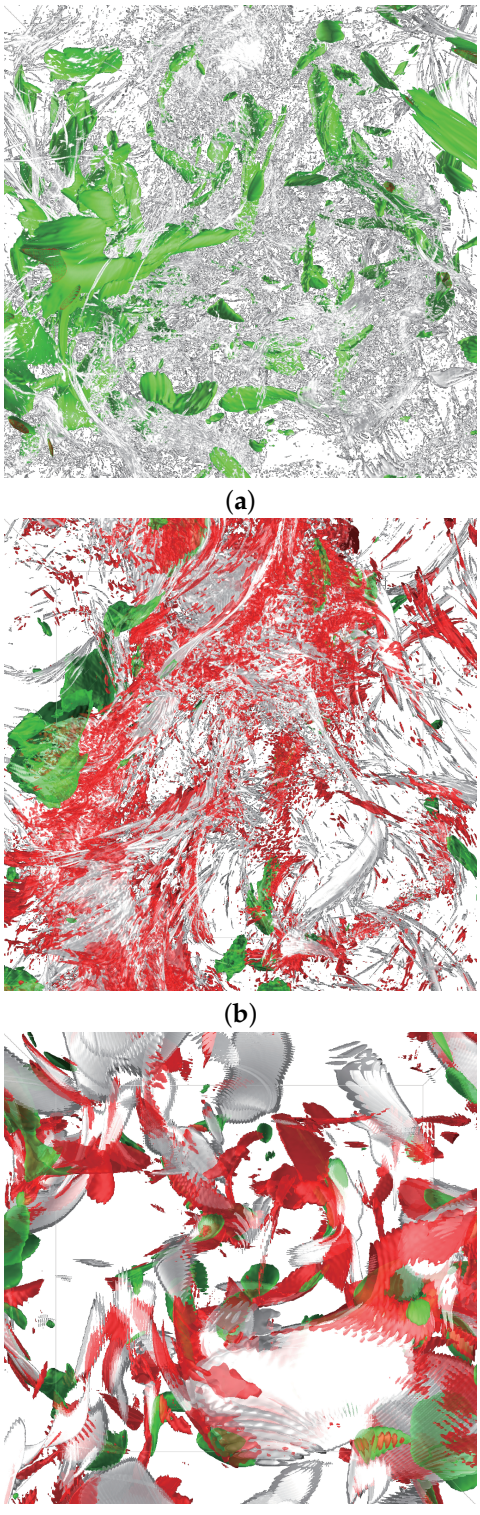

Figure 6. Isosurfaces of E_ω (green) and J (gray) in (**a**) forced Hall MHD turbulence of $Pr_M = 10$ ($\epsilon_H = 0.20, \nu = 1 \times 10^{-3}, \eta = 1 \times 10^{-4}$), (**b**) forced Hall MHD turbulence of $Pr_M = 100$ ($\epsilon_H = 0.20, \nu = 1 \times 10^{-2}$), $\eta = 1 \times 10^{-4}$, and (**c**) forced MHD turbulence of $Pr_M = 100$ ($\epsilon_H = 0, \nu = 1 \times 10^{-2}, \eta = 1 \times 10^{-4}$). Isosurfaces of the palinstrophy density (red) are drawn in (**b**,**c**), whereas they are not drawn in (**a**) for clarity in the figure. Figures are reused from Miura et al. [84], in accordance with the copyright policy of the American Physical Society.

4.3. Energy Transfer and Coherent Structures

Here we consider Hall effects on the coherent or fine structures from the point of view of the energy spectrum. In Figure 7, (a) the kinetic energy spectrum $E_M(k)$ and (b) magnetic energy spectrum in a Hall MHD run ($\epsilon_H = 0.05$, 0.025) and MHD run ($\epsilon_H = 0$) analyzed in Ref. [58] are presented. In order to see the MHD scale ($k < 1/\epsilon_H$) closely, a range of $k < 50$ is presented in the linear–linear plot. (The log–log plot of the full range of the energy spectra can be seen in Ref. [58]). Although Figure 7a does not show a clear difference among the three runs, Figure 7b shows that the large-scale magnetic energy decreases as the Hall parameter ϵ_H becomes larger. Although the current sheet covers a relatively wide range of the wave-number from the largest scale of the inertial range to the dissipation range as pointed out for MHD turbulence [130], the suppression of the magnetic energy at the MHD scale suggests the suppression of the size of the current sheets.

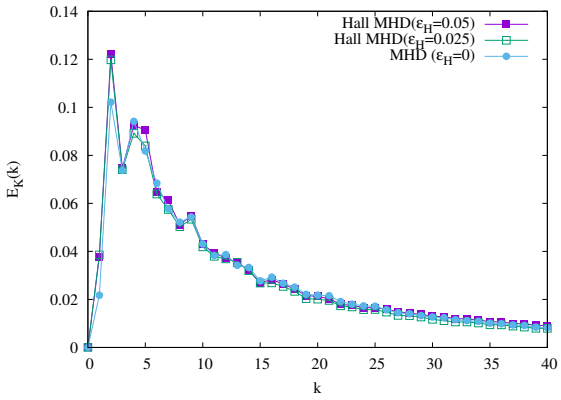

(**a**)

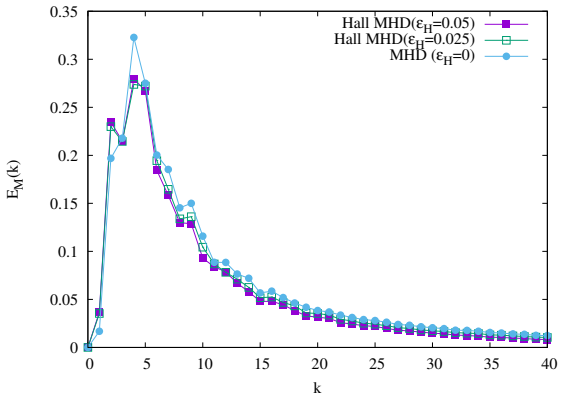

(**b**)

Figure 7. (**a**) The kinetic energy spectrum $E_M(k)$ and (**b**) magnetic energy spectrum in a Hall MHD run ($\epsilon_H = 0.05$ and 0.025) and MHD run ($\epsilon_H = 0$) presented in Ref. [58].

One important bit of information related to the filamentary structure formation, Figures 5 and 6, is found in Ref. [140]. In the literature, the authors have extended an earlier study by Galtier [90] and expressed Hall MHD equations by the generalized Elsässer variable. Then, the nonlinear energy transfer of Equations (1)–(4) is expressed by the couplings of ion–cyclotron (IC) and whistler (Wh) modes. Time series of the energy transfer spectra for the IC and Wh modes in [140] are presented in Figure 8. (The figures are reused from [140]). While an active scale-to-scale energy transfer is observed in both the IC modes and the Wh modes, we can see in the figure that the energy exchange between the two modes is mainly from the IC mode to the Wh mode, and the transfer in the opposite direction is very small. This suggests that the magnetic field excited in the decay of Hall MHD turbulence is going to be occupied by the whistler waves. Since a propagation of a whistler wave forms a spiral magnetic field orbit elongated along a large-scale magnetic

field line, it is natural that the excitation of the whistler wave brings about filamentary structures in a visualization of J.

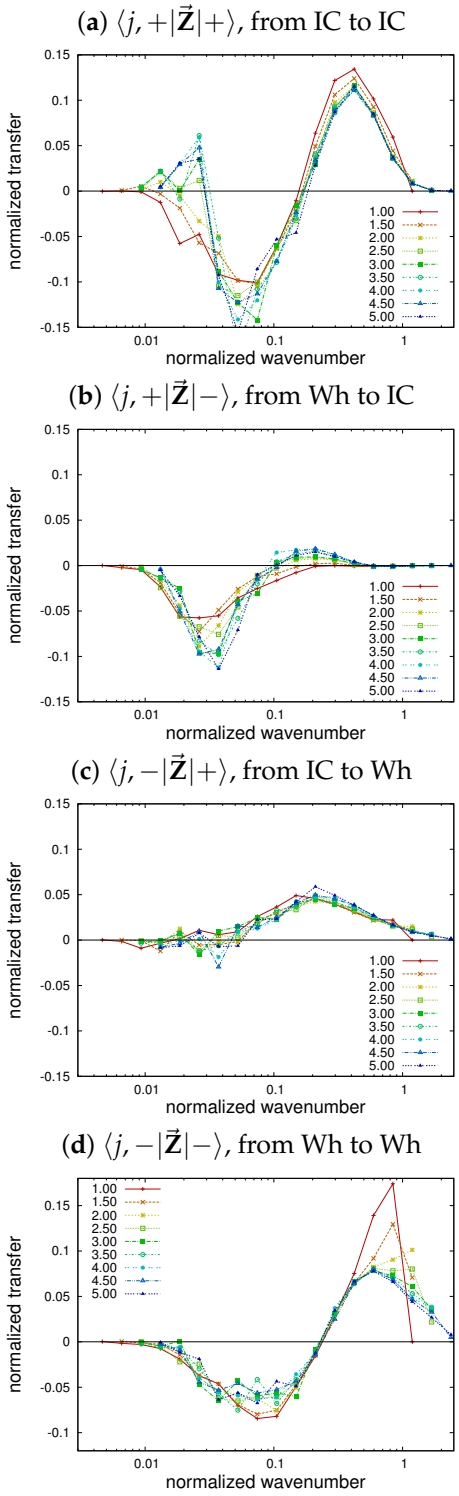

Figure 8. Time series of the ETF spectra for each wave mode, $\langle j, s|\vec{\mathbf{Z}}|s'\rangle$ for $s, s' = \pm 1$. Both the moduli and abscissa are normalized using $\epsilon_B(t)$ and η. Reused from Araki and Miura [140] in accordance with the copyright policy of the Japan Society of Plasma Science and Nuclear Fusion.

This understanding is supported by observing magnetic field vector topology. The presence of elongated spiral magnetic field lines is consistent with the excitation of the whistler mode. We recall that spiral field lines in the velocity field are often visualized by

the use of three invariants of the velocity gradient tensor P, Q, and R [141] (in the case of an incompressible fluid, $P \equiv 0$). The so-called Q-value is used quite frequently to visualize tubular structures in turbulence. In the same manner, we visualize spiral magnetic field vector topology by the use of the three invariants of the magnetic field gradient tensor.

In Figure 9, J (green) and the Q-value of the magnetic field (gray) are drawn in the same simulation as Figure 5b. We find that the two kinds of isosurfaces overlap with each other in the encircled regions. While J (green) tends to be sheet-like, fine structures of the Q-values (gray), which are supposed to arise from the whistler waves, add filamentary variations to the current sheets.

We recall that the $Q - R$ plots of the magnetic and the velocity field vectors in MHD turbulence have been already studied by Sahoo et al. [118] In Figure 10, contours of the joint PDFs of the $Q - R$ values of MHD turbulence with various magnetic Prandtl numbers with or without external forcing, presented in Ref. [118] as Figure 31, are reproduced with permission by the authors and the Institute of Physics. Recently, Yadav et al. have carried out the $Q - R$ analysis of both MHD an Hall MHD turbulence [142]. See Ref. [142] for a comparison of the $Q - R$ plots between MHD and Hall MHD simulations.

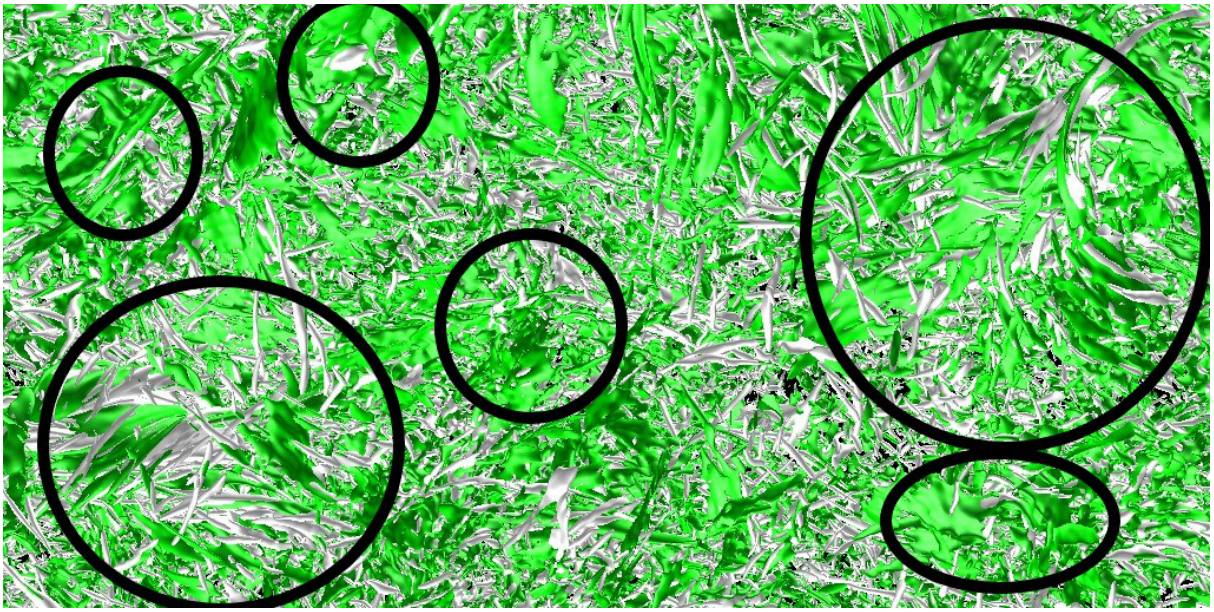

Figure 9. Isosurfaces of J (green) and the Q-value (gray) of the magnetic field in the same simulation as Figure 5.

4.4. Additional Note on Coherent Structures

We add some notes on magnetic reconnection and scientific visualization and on the relationship between intermittency and phenomenology briefly here.

Magnetic reconnection is a representative phenomenon of the dynamic plasma phenomenon. This phenomenon influences turbulence through changing the topology of magnetic field lines. It is considered that the Hall term enhances the magnetic reconnection by thinning a current sheet, although the Hall term itself is not diffusive. In fact, Stawarz and Pouquet have reported that current sheets are finer and thinner in Hall MHD turbulence than in MHD turbulence [138]. There have been an enormous number of studies on this subject, and reviewing magnetic reconnection is outside the scope of this article. See Refs. [44,45,143–154] and references therein for information on turbulent reconnection, including Hall effects.

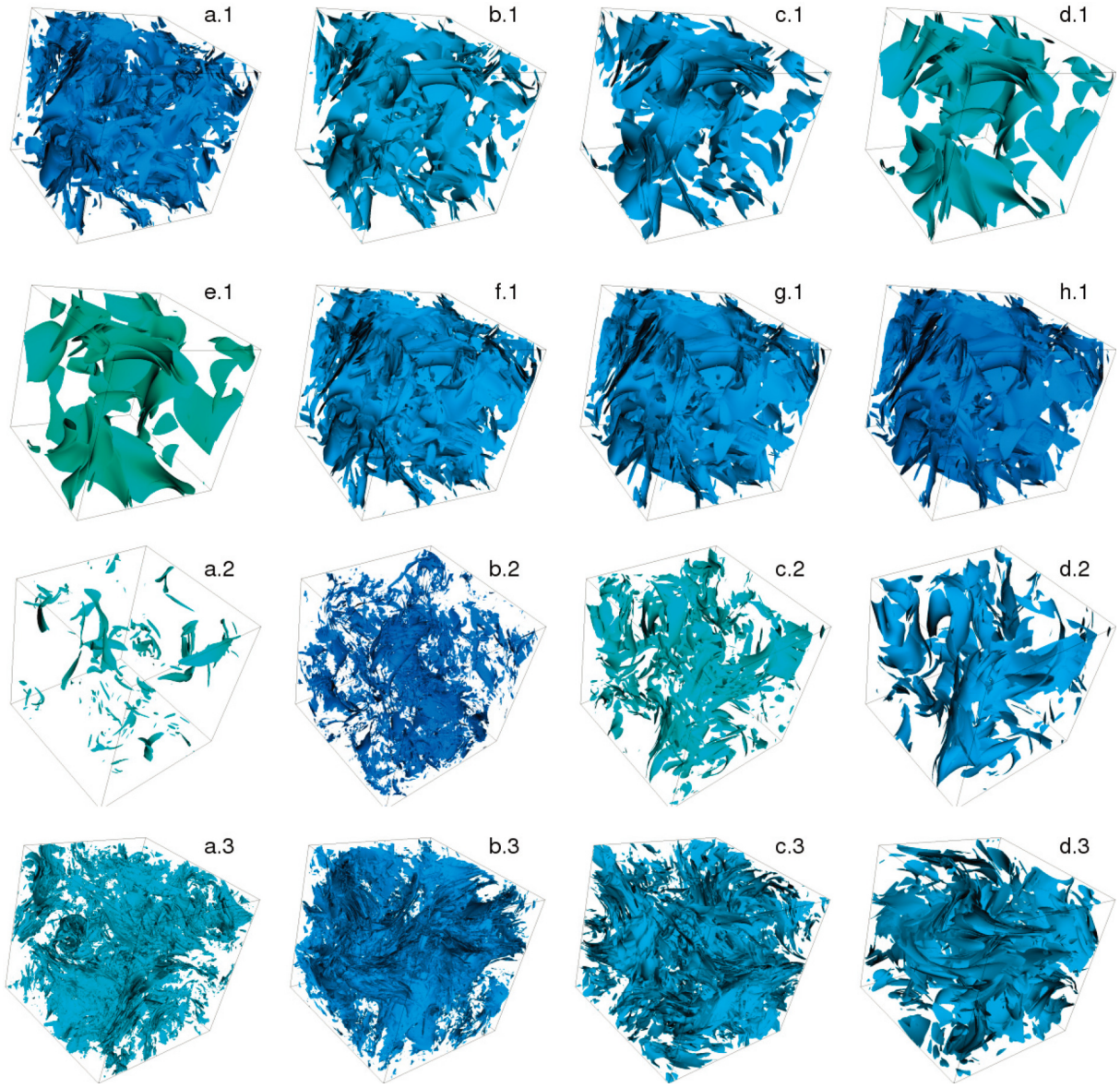

Figure 10. Contours of the joint PDFs of the $Q - R$ values of MHD turbulence with various magnetic Prandtl numbers with and without external forcing. The panels (**a.1**)–(**d.3**) is for different magnetic Prandtl numbers from $Pr_M = 0.1$ to 10.0 and other numerical conditions. See Table 1 of [118] for detailed numerical conditions. Reprinted from Sahoo et al. [118]. © IOP Publishing Ltd. and Deutsche Physikalische Gesellschaft. Reproduced by permission of IOP Publishing. CC BY-NC-SA https://creativecommons.org/licenses/by-nc-sa/3.0/ (accessed on 25 June 2024).

There have been efforts to identify reconnecting current sheets [155,156] and study magnetic field line topology in the current sheets [129], for example. Identifying reconnection events in a large-scale numerical simulation contains multiple steps: identifying the magnetic reconnection point, quantifying the change of the magnetic field topology, quantifying physical impacts of the magnetic reconnection on turbulence, viewing topological change of the magnetic field, and other physical quantities or conditions that are caused by the magnetic reconnection. Since each of the steps is possible, carrying out such processes in a massively parallel computation is not an easy task, and we need to build a new methodological approach to enable such a complex analysis.

For the purpose of visualizing such a complex phenomenon, an in situ visualization approach has been proposed for scientific visualizations [157,158]. One in situ visualization technique, the Four-Dimensional Street View (4DSV) has been implemented to visualize

Hall MHD simulation results [159]. In the 4DSV visualization, many omnidirectional cameras are set to find an extreme event in a simulation. Such an approach may help identify reconnection events and watch formation of coherent structures in Hall MHD simulations.

Formation of coherent or fine structures is also closely related to classic Kolmogorov's and Iroshnikov–Kraichnan's phenomenology as well as to intermittency study by the use of the structure functions. In a strong Kolmogorov turbulence, filamentary current structures and tubular structures are likely to be formed. On the contrary, sheet structures are more usually formed in a simulation that obeys Iroshnikov–Kraichnan phenomenology. These two kinds of phenomenology can be distinguished by studying the scaling exponent ζ_p of the structure function of the Elsässer variable. We expect $\zeta_p \sim p/3$ for the p-th order structure function of Kolmogorov's phenomenology, while we expect $\zeta_p \sim p/4$ for the Iroshnikov–Kraichnan phenomenology [59,88]. Although such a study can be found in earlier works, for example in Ref. [125], a study on Hall MHD turbulence including the sub-ion scale may not yet be sufficient, especially in the context of a fine structure formation. In order to elucidate the physics of formation of coherent structures, we need further studies in relation to phenomenology.

5. Summary

We have seen formation of fine structures in homogeneous and isotropic Hall MHD turbulence simulations. Although many works report the formation of large-scale magnetic field structures (current sheets), the results reviewed in this article show that there are occasions when the Hall term enhances filamentary structures. The enhancement of the fine and filamentary structures in freely decaying Hall MHD simulations reviewed in this article is considered to be due to the almost one-way energy transfer from the ion–cyclotron mode to the whistler mode. The transfer consequently enhances the whistler mode, which appears together with an elongated spiral magnetic field orbit (and thus a filamentary current structure). This may be true for many cases in which the Hall term appears to enhance filamentary structures.

We note that the enhancement of fine or filamentary structures and enhancement of large-scale structures do not necessarily contradict each other. In forced turbulence, there can be an enhancement of the Alfvén mode by an external force and the consequent formation of current sheets, while the energy transfer keeps enhancing the whistler modes at the sub-ion scale. Excitation of small-scale components in the magnetic field can easily mask the presence of the large-scale structures by fine current filaments or fine threads. We need further study to clarify how far the Hall effect can reach the large-scale side of the wave-number space through nonlinear energy transfer and how the Hall term can modify the large-scale structure by nonlinear interaction.

Funding: This research was partially supported by JSPS KAKENHI Grant Numbers 17K05734, 20H00225, and 24K06893, of Japan, and by the NINS program of Promoting Research by Networking among Institutions (Grant Number 01422301).

Acknowledgments: The author would like to thank the authors of the articles whose figures were reused in this article. They kindly sent the author their original figures and other related materials. The numerical simulations were performed on an NEC SX-Aurora TSUBASA A412-8 *Plasma Simulator* at the National Institute of Fusion Science (NIFS), Japan, with the support and under the auspices of the NIFS Collaboration Research program (NIFS23KISS030), FUJITSU FX1000 *Wisteria/BDEC-01 Odyssey* of the University of Tokyo with partial support from the "Joint Usage/Research Center for Interdisciplinary Large-scale Information Infrastructures" (Project ID: jh170009-NAH, jh180003-NAH, jh190006-NAJ, jh200002NAH, jh210004-NAH, jh220005, jh230004, jh240004), and FUJITSU/RIKEN *FUGAKU* with the support of the HPCI System Research Project (Project ID: hp240026) in Japan. The author would like to thank research collaborators K. Araki, T. Gotoh, F. Hamba, A. Kageyama, T. Katagiri, T. Matsumoto, K. Nakajima, N. Ohno, R. Pandit, D. Takahashi, T. Watanabe, and S. K. Yadav, as well as colleagues from the author's institute for fruitful discussions. With respect to numerical simulations, T. Gotoh has kindly allowed to use his FT3D FFT (non-open-source) library. F. Hamba has helped develop an SGS model for Hall MHD turbulence simulations. D. Takahashi has kindly

updated his FFTE library in the course of communication regarding the JHPCN collaboration. K. Nakajima and T. Katagiri have also helped with code development through the JHPCN collaboration. A. Kageyama and N. Ohno have helped develop the data visualization part of the simulation code. The author also would like to thank the software engineers of FUJITSU and NEC, who have helped develop and optimize our simulation code for FX100, FX1000, Fugaku, and SX-Aurora TSUBASA.

Conflicts of Interest: The author declare no confilicts of interest.

Abbreviations

The following abbreviations are used in this manuscript:

DNS	direct numerical simulation
FFT	fast Fourier transform
GS	grid scale
LES	large eddy simulation
SGS	sub-grid scale

Appendix A. Large Eddy Simulation of Hall MHD Model

In order to accommodate a numerical simulation within a finite number of grid points, hyper-diffusivity is often used; however, it is not necessarily a very convenient tool. There is no trivial way of determining the hyper-diffusivity coefficients and the order of the hyper-diffusivity. A serious inconvenience is that the introduction of hyper-diffusivity makes the Hall MHD Equations (1)–(4) very stiff if the coefficients and/or the order of the hyper-diffusivity is large and/or high. Furthermore, since hyper-diffusivity consists of a simple power of the Laplacian of a variable, the hyper-diffusivity operates in the whole region of the computational box. This may cause an unexpected smoothing of a numerical simulation.

In order to avoid such a difficulty with hyper-diffusivity and to compromise the numerical stability as a requirement for the numerical resolution, we may find an alternative approach in LES. Although the LES technique is not frequently used in simulation studies of MHD and Hall MHD turbulence, there are some earlier works that apply the technique to (non-Hall) MHD turbulence [160–163]. See review articles [162,163] for application of an LES of MHD turbulence to space plasma studies.

Miura et al. have recently developed a sub-grid-scale (SGS) model for Hall MHD turbulence simulation [164–166]. An advantage of LES for Hall MHD turbulence is that the dissipation (Smagorinsky) coefficients in the model are determined by the strain rate tensor and J_i in the grid scale (GS) autonomously. The Smagorinsky coefficients are basically determined by considering the energy transfer between the GS and the SGS. The SGS model works as a local and adaptive low-pass filter and smooths a numerical solution only in a region where the numerical solution is going to be very steep. By using this technique, we can avoid the adjustment of the coefficient and unexpected global influence of hyper-diffusivity. Formulation of the LES of Hall MHD turbulence in Refs. [164–166] and the SGS model are presented below.

The GS equations of the Hall MHD system can be described by the use of a low-pass filter (we denote a filtered variable, or a GS variable, by the overbar), as presented in Ref. [164]:

$$\frac{\partial \overline{u}_i}{\partial t} = -\frac{\partial}{\partial x_j}\left[\left(\overline{u}_i\overline{u}_j - \overline{B}_i\overline{B}_j\right) + \left(\overline{p} + \frac{1}{2}\overline{B}_k\overline{B}_k\right)\delta_{ij}\right] + \nu\frac{\partial \overline{S}_{ij}}{\partial x_j} - \frac{\partial \overline{\tau}_{ij}}{\partial x_j}, \tag{A1}$$

$$\overline{\tau}_{ij} = \left[\left(\overline{u_iu_j} - \overline{B_iB_j}\right) + \frac{1}{2}\overline{B_kB_k}\delta_{ij}\right] - \left[\left(\overline{u}_i\overline{u}_j - \overline{B}_i\overline{B}_j\right) + \frac{1}{2}\overline{B}_k\overline{B}_k\delta_{ij}\right], \tag{A2}$$

$$\overline{S}_{ij} = \frac{\partial \overline{u}_i}{\partial x_j} + \frac{\partial \overline{u}_j}{\partial x_i}, \tag{A3}$$

$$\frac{\partial \overline{u}_k}{\partial x_k} = 0, \tag{A4}$$

$$\frac{\partial \overline{B}_i}{\partial t} = -\epsilon_{ijk} \frac{\partial \overline{E}_k}{\partial x_j}, \tag{A5}$$

$$\overline{E}_i = -\epsilon_{ijk} \left(\overline{u}_j - \epsilon_H \overline{J}_j \right) \overline{B}_k + \eta \overline{J}_i - \overline{E}_i^M - \overline{E}_i^H, \tag{A6}$$

$$\overline{E}_i^M = -\epsilon_{ijk} \left(\overline{u_j B_k} - \overline{u}_j \overline{B}_k \right), \tag{A7}$$

$$\overline{E}_i^H = -\epsilon_H \epsilon_{ijk} \left(-\overline{J_j B_k} + \overline{J}_j \overline{B}_k \right), \tag{A8}$$

$$\frac{\partial \overline{B}_k}{\partial x_k} = 0. \tag{A9}$$

In Ref. [164], the SGS terms $\overline{\tau}_{ij}$, $\overline{E}_i^M$, and $\overline{E}_i^H$ have been modeled as:

$$\overline{\tau}_{ij} = -\nu_{SGS} \overline{S}_{ij}, \tag{A10}$$

$$\overline{E}_i^M + \overline{E}_i^H = -\eta_{SGS} \overline{J}_i, \tag{A11}$$

$$\nu_{SGS} = C_\nu \Delta^2 \left(\frac{1}{2} C_\nu \overline{S}_{ij}^2 + C_\eta \overline{J}_i^2 \right)^{1/2}, \tag{A12}$$

$$\eta_{SGS} = C_\eta \Delta^2 \left(\frac{1}{2} C_\nu \overline{S}_{ij}^2 + C_\eta \overline{J}_i^2 \right)^{1/2}. \tag{A13}$$

Here, the symbol Δ is the truncation width of a low-pass filter. The two diffusive (Smagorinsky) coefficients C_ν and C_η are given theoretically in Ref. [161], although we need to carry out some simulations to calibrate the coefficients.

In the newest SGS model for Hall MHD turbulence in Ref. [165], $\overline{E}_i^M$ and $\overline{E}_i^H$ are modeled as:

$$\overline{E}_i^M + \overline{E}_i^H = -\eta_{SGS} \overline{J}_i + \epsilon_H \frac{\partial}{\partial x_j} \left(\nu_{SGS} \sigma_{H,1} \overline{S}_{ij} \right) - \epsilon_H^2 \frac{\partial}{\partial x_j} \left[\nu_{SGS} \sigma_{H,2} \overline{S}_{ij} \left(\frac{\partial \overline{J}_i}{\partial x_j} + \frac{\partial \overline{J}_j}{\partial x_i} \right) \right]. \tag{A14}$$

In Ref. [165], an LES with the set of parameters $\Delta = 1.5\Delta_0$ (Δ_0 is the grid width), $C_\nu = 0.0535$, and $C_\eta = 0.0382$ have shown good agreement with spectra as well as PDFs of E_ω and J with DNS results.

It has been shown in Ref. [165] that an LES of Hall MHD turbulence can reproduce statistical properties of turbulence fields such as energy spectra and PDFs of E_ω and J, not only for homogeneous and isotropic turbulence but also for homogeneous turbulence with a guiding uniform and constant magnetic field, while the computational cost of an LES can be suppressed to 1/512 (in the best case) of that of a direct numerical simulation (DNS). It has also been shown there that fine coherent structures observed in DNS can be reasonably reproduced in an LES.

We note that there are some formulations and methods of LES other than those shown above. Regarding structures in real space, either a scale similarity model, dynamic Smagorinsky model, or a mixed-scale one is known to reproduce DNS results well [167]. A dynamic Smagorinsky model has been used by Chernyshov et al. [162]. This is because the formulation in Ref. [161] puts a higher priority on the energy budget between the GS and SGS components than to the reproduction of structures in real space. However, it has been shown in Refs. [164,165] that the SGS models above can reproduce coherent structures if the Smagorinsky coefficients are calibrated carefully. Furthermore, an SGS model based on the formulation given in Ref. [161] is flexible and applicable to the extension of the Hall

MHD equations. For example, in Ref. [164], the SGS model has been applied to simulations of extended MHD equations with gyro-viscosity (finite Larmor radius effects). Since we sometimes need to extend the equations to the effects of scale length that are shorter than the ion-skin-depth, the flexibility of the formulation can be a great advantage.

In the context of study of physics, we can replace some parts of the sub-ion scale with the SGS model and use a considerable part of the numerical resolution in our simulation to resolve the MHD scale. Then, we can keep a bandwidth of the MHD-scale in Hall MHD simulation as wide as (non-Hall) MHD simulation, while the Hall effects can be represented by the SGS model. Since an LES study of Hall MHD turbulence has just begun, we need further study regarding the Hall effects on the MHD scale by comparing the LES results to DNS results, and then updating the SGS model as necessary.

References

1. Braginskii, S.I. Transport processes in a plasma. In *Reviews of Plasma Physics*; Leontovich, M.A., Ed.; Consultants Bureau: New York, NY, USA, 1965; Volume 1, p. 205.
2. Holm, D.D. Hall magnetohydrodynamics: Conservation laws and Lyapunov stability. *Phys. Fliuds* **1987**, *30*, 1310. [CrossRef]
3. Mahajan, S.M.; Yoshida, Z. Double Curl Beltrami Flow: Diamagnetic Structures. *Phys. Rev. Lett.* **1998**, *81*, 4863. [CrossRef]
4. Saharoui, F.; Belmont, G.; Rezeau, L. Hamiltonian canonical formulation of Hall-magnetohydrodynamics: Toward an application to weak turbulence theory. *Phys. Plasmas* **2003**, *10*, 1325.
5. Yoshida, Z.; Mahajan, S.M.; Ohsaki, S. Scale hierarchy created in plasma flow. *Phys. Plasmas* **2004**, *11*, 3660. [CrossRef]
6. Ohsaki, S.; Mahajan, S.M. Hall current and Alfvén wave. *Phys. Plasmas* **2004**, *11*, 898. [CrossRef]
7. Krishnan, V.; Mahajan, S.M. Magnetic fluctuations and Hall magnetohydrodynamic turbulence in the solar wind. *J. Geophys. Res.* **2004**, *109*, A11.
8. Hameiri, E.; Torasso, R. Linear stability of static equilibrium states in the Hall-magnetohydrodynamics model. *Phys. Plasmas* **2004**, *11*, 4394. [CrossRef]
9. Hirota, M.; Yoshida, Z.; Hameiri, E. Variational principle for linear stability of flowing plasmas in Hall magnetohydrodynamics. *Phys. Plasmas* **2006**, *13*, 022107. [CrossRef]
10. Mahajan, S.M. Classical Perfect Diamagnetism: Expulsion of Current from the Plasma Interior. *Phys. Rev. Lett*. **2008**, *100*, 075001. [CrossRef]
11. Shivamoggi, B.K. Impulse formulations of Hall magnetohydrodynamic equations. *Phys. Lett. A* **2009**, *373*, 708. [CrossRef]
12. Eyink, G.L. Stochastic line motion and stochastic flux conservation for nonideal hydromagnetic models. *J. Math. Phys.* **2009**, *50*, 083102. [CrossRef]
13. Araki, K. Helicity-based particle-relabeling operator and normal mode expansion of the dissipationless incompressible Hall magnetohydrodynamics. *Phys. Rev. E* **2015**, *92*, 063106. [CrossRef] [PubMed]
14. Araki, K. Differential-geometrical approach to the dynamics of dissipationless incompressible Hall magnetohydrodynamics: I. Lagrangian mechanics on semidirect product of two volume preserving diffeomorphisms and conservation laws. *J. Phys. A Math. Theor.* **2015**, *48*, 175501. [CrossRef]
15. Mahajan, S.; Miura, H. Linear superposition of nonlinear waves. *J. Plasma Phys.* **2009**, *75* 145. [CrossRef]
16. Abdelhamid, H.M.; Lingam, M.; Mahajan, S.M. Extended MHD turbulence and its applications to the solar wind. *Astrophys. J.* **2016**, *829*, 87. [CrossRef]
17. D'Avignon, E.D.; Morrison, P.; Lingam, M. Derivation of the Hall and extended magnetohydrodynamics brackets. *Phys. Plasmas* **2016**, *23*, 062101. [CrossRef]
18. Araki, K. Differential-geometrical approach to the dynamics of dissipationless incompressible Hall magnetohydrodynamics: II. Geodesic formulation and Riemannian curvature analysis of hydrodynamic and magnetohydrodynamic stabilities. *J. Phys. A Math. Theor.* **2017**, *50*, 235501. [CrossRef]
19. Kawazura, Y.; Miloshvich, G.; Morrison, P. Action principles for relativistic extended magnetohydrodynamics: A unified theory of magnetofluid models. *Phys. Plasmas* **2017**, *24*, 022103. [CrossRef]
20. Miloshevich, G.; Lingam, M.; Morrison, P.J. On the structure and statistical theory of turbulence of extended magnetohydrodynamics. *New J. Phys.* **2017**, *19*, 015007. [CrossRef]
21. Bello-Beneítez, E.; Sánchez-Arriaga, G.; Passot, T.; Laveder, D.; Siminos, E. Structure and evolution of magnetohydrodynamic solivary waves with Hall and finite Larmor radius effects. *Phys. Rev. E* **2019**, *99*, 023202. [CrossRef]
22. Rosenbluth, M.N.; Krall, N.A.; Rostoker, N. Finite larmor radius stabilization of "Weakly" unstable confined plasmas. *Nucl. Fusion Suppl.* **1962**, *1*, 143.
23. Roberts, K.V.; Taylor, J.B. Magnetohydrodynamic Equations for Finite Larmor Radius. *Phys. Rev. Lett.* **1962**, *8*, 197. [CrossRef]
24. Huba, J.D. Finite Larmor radius magnetohydrodynamics of the Rayleigh-Taylor instability. *Phys. Plasmas* **1996**, *3*, 2523. [CrossRef]
25. Winske, D. Regimes of the magnetized Rayleigh-Taylor instability. *Phys. Plasmas* **1996**, *3*, 11. [CrossRef]
26. Huba, J.D.; Winske, D. Rayleigh-Taylor instability: Comparison of hybrid and nonideal magnetohydrodynamic simulations. *Phys. Plasmas* **1998**, *5*, 2305. [CrossRef]

27. Chacon, L.; Knoll, D.A.; Finn, J.M. Hall MHD effects on the 2D Kelvin-Helmholtz/tearing instability. *Phys. Lett. A* **2003**, *308*, 187. [CrossRef]
28. Filippychev, D.S. Simulation of space plasma allowing for the Hall effect: Kelvin-Helmholtz and Rayleigh-Taylor instabilities. *Comput. Math. Model.* **2006**, *17*, 140. [CrossRef]
29. Zhu, P.; Schnack, D.D.; Ebrahimi, F.; Zweibel, E.G.; Suzuki, M.; Hegna, C.C.; Sovinec, C.R. Absence of Complete Finite-Larmor-Radius Stabilization in Extended MHD. *Phys. Rev. Lett.* **2008**, *101*, 085005. [CrossRef]
30. Ebrahimi, F.; Lefebvre, B.; Forest, C.B.; Bhattacharjee, A. Global Hall-MHD simulations of magnetorotational instability in a plasma Couette flow experiment. *Phys. Plasmas* **2011**, *18*, 062904. [CrossRef]
31. Ahedo, E.; Ramos, J.J. Supersonic regime of the Hall-magnetohydrodynamics resistive tearing instability. *Phys. Plasmas* **2012**, *19*, 072519. [CrossRef]
32. Xi, P.W.; Xu, X.Q.; Xia, T.Y.; Nevins, W.M.; Kim, S.S. Impact of a large density gradient on linear and nonlinear edge-localized mode simulations. *Nucl. Fusion* **2013**, *53*, 113020. [CrossRef]
33. Goto, R.; Miura, H.; Ito, A.; Sato, M.; Hatori, T. Hall and Gyro-Viscosity Effects on the Rayleigh-Taylor Instability in a 2D Rectangular Slab. *Plasma Fusion Res.* **2014**, *9*, 1403076. [CrossRef]
34. Goto, R.; Miura, H.; Ito, A.; Sato, M.; Hatori, T. Formation of large-scale structures with sharp density gradient through Rayleigh-Taylor growth in a two-dimensional slab under the two-fluid and finite Larmor radius effects. *Phys. Plasmas* **2015**, *22*, 032115. [CrossRef]
35. Ghosh, S.; Parashar, T. Linear vs. nonlinear acceleration in plasma turbulence. II. Hall–finite-Larmor-radius magnetohydrodynamics. *Phys. Plasmas* **2015**, *22*, 042303. [CrossRef]
36. Lu, H.Y.; Cao, J.B.; Ge, Y.S.; Zhang, T.L.; Nakamura, R.; Dunlop, M.W. Hall and finite Larmor radius effects on the dipolarization fronts associated with interchange instability. *Geophys. Res. Lett.* **2015**, *42*, 10099–10105. [CrossRef]
37. Ito, A.; Miura, H. Parameter dependence of two-fluid and finite Larmor radius effects on the Rayleigh-Taylor instability in finite beta plasmas. *Phys. Plasmas* **2016**, *23*, 122123. [CrossRef]
38. Umeda, T.; Wada, Y. Non-MHD effects in the nonlinear development of the MHD-scale Rayleigh-Taylor instability. *Phys. Plasmas* **2017**, *24*, 072307. [CrossRef]
39. Mininni, P.D.; Gómez, D.O.; Mahajan, S.M. Dynamo action in magnetohydrodynamics and Hall-magnetohydrodynamics. *Astrophys. J.* **2003**, *587*, 472. [CrossRef]
40. Mininni, P.; Gómez, D.O.; Mahajan, S. Role of the Hall current in magnetohydrodynamic dynamos. *Astrophys. J.* **2003**, *584*, 1120. [CrossRef]
41. Matthaeus, W.H.; Dmitruk, P.; Smith, D.; Ghosh, S.; Oughton, S. Impact of Hall effect on energy decay in magnetohydrodynamic turbulence. *Geophys. Res. Lett.* **2003**, *30*, 2104. [CrossRef]
42. Mininni, P.D.; Gómez, D.O.; Mahajan, S.M. Direct numerical simulations of helical Hall-MHD turbulence and dynamo action. *Astrophys. J.* **2005**, *619*, 1019. [CrossRef]
43. Halder, A.; Banerjee, S.; Chatterjee, A.G.; Sharma, M.K. Contribution of the Hall term in small-scale magnetohydrodynamic dynamos. *Phys. Rev. Fluids* **2023**, *8*, 053701. [CrossRef]
44. Kerr, R.M.; Brandenburg, A. Evidence for a Singularity in Ideal Magnetohydrodynamics: Implications for Fast Recon-nection. *Phys. Rev. Lett.* **1999**, *83*, 1155. [CrossRef]
45. Eyink, G.L.; Lazarian, A.; Vishniac, E.T. Fast magnetic reconnection and spontaneous stochasticity. *Astrophys. J* **2011**, *743*, 51. [CrossRef]
46. Karimabadi, H.; Roytershteyn, V.; Wan, M.; Matthaeus, W.H.; Daughton, W.; Wu, P.; Shay, M.; Loring, B.; Borovsky, J.; Leonardis, E.; et al. Coherent structures, intermittent turbulence, and dissipation in high-temperature plasmas. *Phys. Plasmas* **2013**, *20*, 012303. [CrossRef]
47. Krauss-Varban, D.; Omidi, N.; Quest, K.B. Mode properties of low-frequency waves, Kinetic theory versus Hall-MHD. *J. Geophys. Res.* **1994**, *99*, 5987–6009. [CrossRef]
48. Schnack, D.D.; Barnes, D.C.; Brennan, D.P.; Hegna, C.C.; Held, E.; Kim, C.C.; Kruger, S.E.; Pankin, A.Y.; Sovinec, C.R. Computational modeling of fully ionized magnetized plasmas using the fluid approximation. *Phys. Plasmas* **2006**, *13*, 058103. [CrossRef]
49. Schnack, D.D.; Cheng, J.; Barnes, D.C.; Parker, S.E. Comparison of kinetic and extended magnetohydrodynamics computational models for the linear ion temperature gradient instability in slab geometry. *Phys. Plasmas* **2013**, *20*, 062106. [CrossRef]
50. Papini, E.; Franci, L.; Landi, S.; Verdini, A.; Matteini, L.; Helinger, P. Can Hall Magnetohydrodynamics Explain Plasma Turbulence at Sub-ion Scales. *Astrophys. J.* **2019**, *870*, 52. [CrossRef]
51. Polygiannakis, J.M.; Moussas, X. A review of magneto-vorticity induction in Hall-MHD plasmas. *Plasma Phys. Control. Fusion* **2001**, *43*, 195. [CrossRef]
52. Gomez, D. Parallel Simulations of Hall-MHD Plasmas. *Space Sci. Rev.* **2006**, *122*, 231. [CrossRef]
53. Servidio, S.; Dmitruk, P.; Greco, A.; Wan, M.; Donato, S.; Cassak, P.A.; Shay, M.A.; Carbone, V.; Matthaeus, W.H. Magnetic reconnection as an element of turbulence. *Nonlinear Proc. Geophy.* **2011**, *18*, 675. [CrossRef]
54. Pouquet, A.; Rosenberg, D.; Stawarz, J.E.; Marino, R. Helicity Dynamics, Inverse, and Bidirectional Cascades in Fluid and Magnetohydrodynamic Turbulence: A Brief Review. *Earth Space Sci.* **2019**, *6*, 351. [CrossRef]

55. Pouquet, A.; Yokoi, N. Helical fluid and (Hall)-MHD turbulence: A brief review. *Phil. Trans. R. Soc. A* **2022**, *380*, 38020210087. [CrossRef]
56. Marino, R.; Sorriso-Valvo, L. Scaling laws for the energy transfer in space plasma turbulence. *Phys. Rep.* **2023**, *1006*, 1. [CrossRef]
57. Miura, H.; Araki, K. Coarse-graining study of homogeneous and isotropic Hall magnetohydrodynamics turbulence. *Plasma Phys. Control. Fusion* **2013**, *55*, 014012. [CrossRef]
58. Miura, H.; Araki, K. Structure transitions induced by the Hall term in homogeneous and isotropic magnetohydrodynamic turbulence. *Phys. Plasmas* **2014**, *21*, 072313. [CrossRef]
59. Biskamp, D. *Magnetohydrodynamic Turbulence*; Cambridge University Press: Cambridge, UK, 2003.
60. Davidson, P.A. *Turbulence*; Cambridge University Press: Cambridge, UK, 2004.
61. Davidson, P.A. *Turbulence in Rotating, Stratified and Electrically Conducting Fluids*; Cambridge University Press: Cambridge, UK, 2013.
62. Alexandrova, O.; Lacombe, C.; Saur, J.; Mangeney, A.; Mitchell, J.; Schwartz, S.J.; Robert, P. Universality of Solar-Wind Turbulent Spectrum from MHD to Electron Scales. *Phys. Rev. Lett.* **2009**, *103*, 165003. [CrossRef]
63. Kiyani, K.H.; Chapman, S.C.; Khotyaintsev, Y.V.; Dunlop, M.W.; Sahraoui, F. Global scale-invariant dissipation in collisionless plasma turbulence. *Phys. Rev. Lett.* **2009**, *103*, 075006. [CrossRef]
64. Bandyopadhyay, R.; Matthaeus, W.H.; McComas, D.J.; Chhiber, R.; Usmanov, A.V.; Huang, J.; Livi, R.; Larson, D.E.; Kasper, J.C.; Case, A.W. Sub-Alfvénic Solar Wind Observed by the Parker Solar Probe: Characterization of Turbulence, Anisotropy, Intermittency, and Switchback. *Astrophys. J. Lett.* **2022**, *926*, L1. [CrossRef]
65. Huang, S.Y.; Xu, S.B.; Zhang, J.; Sahraoui, F.; Andrés, N.; He, J.S.; Yuan, Z.G.; Deng, X.H.; Jiang, K.; Wei, Y.Y.; et al. Anisotropy of Magnetic Field Spectra at Kinetic Scales of Solar Wind. *Turbul. Reveal. Park. Sol. Probe Inn. Heliosphere Astrophys. J. Lett.* **2022**, *929*, L6.
66. Parashar, T.N.; Matthaeus, W.H. Observations of cross scale energy transfer in the inner heliosphere by Parker Solar Probe. *Rev. Mod. Plasma Phys.* **2022**, *6*, 41. [CrossRef] [PubMed]
67. Zhao, L.-L.; Zank, G.P.; Adhikari, L.; Telloni, D.; Stevens, M.; Kasper, J.C.; Bale, S.D.; Raouafi, N.E. Turbulence and Waves in the Sub-Alfvénic Solar Wind Observed by the Parker Solar Probe during Encounter 10. *Astrophys. J. Lett.* **2022**, *934*, L36. [CrossRef]
68. Raouafi, N.E.; Matteini, L.; Squire, J.; Badman, S.T.; Velli, M.; Klein, K.G.; Chen, C.H.K.; Matthaeus, W.H.; Szabo, A.; Linton, M.; et al. Parker Solar Probe: Four Years of Discoveries at Solar Cycle Minimum. *Space Sci. Rev.* **2023**, *219*, 8. [CrossRef]
69. Goldreich, P.; Sridhar, S. Magnetohydrodynamic turbulence revisited. *Astrophys. J.* **1997**, *485* 680. [CrossRef]
70. Galtier, S.; Nazarenko, S.V.; Newell, A.C.; Pouquet, A. A weak turbulence theory for incompressible magnetohydrodynamics. *J. Plasma Phys.* **2000**, *63*, 447. [CrossRef]
71. Cho, J.; Laarian, A. Compressible Sub-Alfvénic MHD Turbulence in Low-b Plasmas. *Phys. Rev. Lett.* **2002**, *88*, 245001. [CrossRef]
72. Cho, J.; Lazarian, A.; Vishniac, E.T. Simulations of magnetohydrodynamic turbulence in a strongly magnetized medium. *Astrophys. J.* **2002**, *564*, 291. [CrossRef]
73. Boldyrev, S. On the spectrum of magnetohydrodynamic turbulence. *Astrophys. J.* **2005**, *636*, L37. [CrossRef]
74. Beresnyak, A.; Lazarian, A. Polarization intermittency and its influence on MHD turbulence. *Astrophys. J.* **2006**, *640*, L175. [CrossRef]
75. Mason, J.; Cattaneo, F.; Boldyrev, S. Numerical measurements of the spectrum in magnetohydrodynamic turbulence. *Phys. Rev. E* **2008**, *77*, 036403. [CrossRef] [PubMed]
76. Boldyrev, S.; Perez, J.C.; Boravsky, J.E.; Podesta, J.J. Specral scaling-laws in magnetohydrodynamic turbulence simulations and in the solar wind. *Astrophys. J. Lett.* **2011**, *741*, L19. [CrossRef]
77. Galtier, S.; Buchlin, E. Multiscale Hall-Magnetohydrodynamic Turbulence in the Solar Wind. *J. Astrophys.* **2007**, *656*, 560–566. [CrossRef]
78. Hori, D.; Miura, H. Spectrum properties of Hall MHD turbulence. *Plasma Fusion Res.* **2008**, *3*, S1053. [CrossRef]
79. Servidio, S.; Matthaeus, W.H.; Shay, M.A.; Cassak, P.A.; Dmitruk, P. Magnetic reconnection in two-dimensional magnetohydrodynamic turbulence. *Phys. Rev. Lett.* **2009**, *102*, 115003. [CrossRef]
80. Galtier, S. Turbulence in space plasma and beyond. *J. Phys.A Math. Theor.* **2018**, *51*, 293001. [CrossRef]
81. Miura, H. Extended Magnetohydrodynamic Simulations of Decaying, Homogeneous, Approximately-Isotropic and Incompressible Turbulence. *Fluids* **2019**, *4*, 46. [CrossRef]
82. Mininni, P.; Alexakis, A.; Pouquet, A. Energy transfer in Hall-MHD turbulence: Cascades, backscatter, and dynamo action. *J. Plasma Phys.* **2007**, *73*, 377. [CrossRef]
83. Meyrand, R.; Galtier, S. Anomalous $k_{\perp}^{-8/3}$ Spectrum in Electron Magnetohydrodynamic Turbulence. *Phys. Rev. Lett.* **2013**, *111*, 264501. [CrossRef]
84. Miura, H.; Yang, J.; Gotoh, T. Hall magnetohydrodynamic turbulence with a magnetic Prandtl number larger than unity. *Phys. Rev. E* **2019**, *100*, 063207. [CrossRef]
85. Takahashi, D. An Implementation of Parallel 1-D FFT Using SSE3 Instructions on Dual-Core Processors. In *Applied Parallel Computing, State of the Art in Scientific Computing. PARA 2006*; Lecture Notes in Computer Science; Springer: Berlin/Heidelberg, Germany, 2007; Volume 4699.
86. Pekurovsky, D. P3DFFT: A framework for parallel computations of Fourier transforms in three dimensions. *SIAM J. Sci. Comput.* **2012**, *34*, C192. [CrossRef]

87. Gotoh, T.; Watanabe, T. Power and Nonpower Laws of Passive Scalar Moments Convected by Isotropic Turbulence. *Phys. Rev. Lett.* **2015**, *115*, 114502. [CrossRef] [PubMed]
88. Politano, H.; Pouquet, A. Model of intermittency in magnetohydrodynamic turbulence. *Phys. Rev. E* **1995**, *52*, 636. [CrossRef] [PubMed]
89. Politano, H.; Pouquet, A. Von Kármán–Howarth equation for magnetohydrodynamics and its consequences on third-order longitudinal structure and correlation functions. *Phys. Rev. E* **1998**, *57*, R21. [CrossRef]
90. Bigot, B.; Galtier, S.; Politano, H. Development of anisotropy in incompressible magnetohydrodynamic turbulence. *Phys. Rev. E* **2008**, *78*, 066301. [CrossRef]
91. Yoshimatsu, K. Examination of the four-fifth law for longitudinal third-order moments in incompressible magnetohydrodynamic turbulence in a periodic box. *Phys. Rev. E* **2012**, *85*, 066313. [CrossRef]
92. Basu, A.; Naji, A.; Pandit, R. Structure-function hierarchies and von Karmán–Howarth relations for turbulence in magnetohydrodynamical equations. *Phys. Rev. E* **2014**, *89*, 012117. [CrossRef]
93. Luo, Q.Y.; Wu, D.J. Observations of anisotropic scaling of solar wind turbulence. *Astrophys. J. Lett.* **2010**, *714*, L138. [CrossRef]
94. Palacios1, J.C.; Bourouaine, S.; Perez, J.C. On the Statistics of Elsasser Increments in Solar Wind and Magnetohydrodynamic Turbulence. *Astrophys. J. Lett.* **2022**, *940*, L20. [CrossRef]
95. Ferrand, R.; Galtier, S.; Sahraoui, F. A compact exact law for compressible isothermal Hall magnetohydrodynamic turbulence. *J. Plasma Phys.* **2021**, *87*, 905870220. [CrossRef]
96. Ferrand, R.; Sahraoui, F.; Galtier, S.; Andrés, N.; Mininni, P.; Dmitruk, P. An In-depth Numerical Study of Exact Laws for Compressible Hall Magnetohydrodynamic Turbulence. *Astrophys. J.* **2022**, *927*, 205. [CrossRef]
97. Wu, H.; Huang, S.; Wang, X.; Yuan, Z.; He, J.; Yan, L. Intermittency of Magnetic Discontinuities in the Near-Sun Solar Wind Turbulence. *Astrophys. J. Lett.* **2023**, *947*, L22. [CrossRef]
98. Banerjee, S.; Galtier, S. Chiral exact relations for helicities in Hall magnetohydrodynamic turbulence. *Phys. Rev. E* **2016**, *93*, 033120. [CrossRef] [PubMed]
99. Hellinger, P.; Verdini, A.; Landi, S.; Franci, L.; Matteini, L. Von Kármán–Howarth Equation for Hall Magnetohydrodynamics: Hybrid Simulations. *Astrophys. J. Lett.* **2018**, *857*, L19. [CrossRef]
100. Andrés, N.; Galtier, S.; Sahraoui, F. Exact law for homogenenous compressible Hall magnetohydrodynamic turbulence. *Phys. Rev. E* **2018**, *97*, 013204. [CrossRef]
101. Andrés, N.; Sahraoui, F.; Galtier, S.; Hadid, L.Z.; Ferrand, R.; Huang, S.Y. Energy Cascade Rate Measured in a Collisionless Space Plasma with MMS Data and Compressible Hall Magnetohydrodynamic Turbulence Theory. *Phys. Rev. Lett.* **2019**, *123*, 245101. [CrossRef]
102. Ferrand, R.; Galtier, S.; Sahraoui, F.; Meyrand, R.; Andrés, N.; Banerjee, S. On Exact Laws in Incompressible Hall Magnetohydrodynamic Turbulence. *Astrophys. J.* **2019**, *881*, 50. [CrossRef]
103. Ishida, T.; Kaneda, Y. Small-scale anisotropy in magnetohydrodynamic turbulence under a strong uniform magnetic field. *Phys. Fluids* **2007**, *19*, 075104. [CrossRef]
104. Mininni, P.D.; Pouquet, A.G.; Montgomery, D.C. Small-Scale Structures in Three-Dimensional Magnetohydrodynamic Turbulence. *Phys. Rev. Lett.* **2006**, *97*, 244503. [CrossRef]
105. Dmitruk, P.; Matthaeus, W.H. Structure of the electromagnetic field in three-dimensional Hall magnetohydrodynamic turbulence. *Phys. Plasmas* **2006**, *13*, 042307. [CrossRef]
106. Araki, K.; Miura, H. Nonlocal Interaction of Inverse Magnetic Energy Transfer in Hall Magnetohydrodynamic Turbulence. *Plasma Fusion Res.* **2011**, *6*, 2401132. [CrossRef]
107. Martin, L.N.; Dmitruk, P.; Gomez, D.O. Energy spectrum, dissipation, and spatial structures in reduced Hall magnetohydrodynamic. *Phys. Plasmas* **2012**, *19*, 052305. [CrossRef]
108. Araki, K.; Miura, H. Generalized Elsässer Energy Spectra of the Ion Cyclotron and whistler Modes in Magnetohydrodynamic and Hall Magnetohydrodynamic Turbulence. *Plasma Fusion Res.* **2015**, *10*, 3401030. [CrossRef]
109. Verma, M.K. Anisotropy in Quasi-Static Magnetohydrodynamic Turbulence. *Rep. Prog. Phys.* **2017**, *80*, 087001. [CrossRef] [PubMed]
110. Galtier, S. On the origin of the energy dissipation anomaly in (Hall) magnetohydrodynamics. *J. Phys. A Math. Theor.* **2018**, *51*, 205501. [CrossRef]
111. Pouquet, A.; Rosenberg, D.; Stawarz, J.E. Interplay between turbulence and waves: Large-scale helical transfer, and small-scale dissipation and mixing in fluid and Hall-MHD. *Rend. Lincei Sci. Fis. Nat.* **2020**, *31*, 949. [CrossRef]
112. Papini, E.; Hellinger, P.; Verdini, A.; Landi, S.; Franci, L.; Montagud-Camps, V.; Matteini, L. Properties of Hall-MHD Turbulence at Sub-Ion Scales: Spectral Transfer Analysis. *Atmosphere* **2021**, *12*, 1632. [CrossRef]
113. Manzini, D.; Califano, F.S.F.; Ferrand, R. Local energy transfer and dissipation in incompressible Hall magnetohydrodynamic turbulence: The coarse-graining approach. *Phys. Rev. E* **2022**, *106*, 035202. [CrossRef]
114. Yoshida, K.; Arimitsu, T. Inertial-subrange structures of isotropic incompressible magnetohydrodynamic turbulence in the Lagrangian renormalized approximation. *Phys. Plasmas* **2007**, *19*, 045106. [CrossRef]
115. Burlaga, L.F. Intermittent turbulence in large-scale velocity fluctuations at 1 AU near solar maximum. *J. Geophys. Res.* **1993**, *98*, 17467. [CrossRef]

116. Alexandrova, O.; Mangeney, A.; Maksimovic, M.; Cornilleau-Wehrlin, N.; Bosqued, J.-M.; André, M. Alfvén vortex filaments observed in magnetosheath downstream of a quasi-perpendicular bow shock. *J. Geophys. Res.* **2006**, *111*, A12208. [CrossRef]
117. Malapaka, S.K.; Müller, W.-C. Large-scale magnetic structure formation in three-dimensional magnetohydrodynamic turbulence. *Astrophys. J.* **2013**, *778*, 21. [CrossRef]
118. Sahoo, G.; Perlekar, P.; Pandit, R. Systematics of the magnetic-Prandtl-number dependence of homogeneous, isotropic magnetohydrodynamic turbulence. *New J. Phys.* **2011**, *13*, 013036. [CrossRef]
119. Verma, M.K. Statistical theory of magnetohydrodynamic turbulence: Recent results. *Phys. Rep.* **2004**, *401*, 229. [CrossRef]
120. Brandenburg, A.; Nordlund, A. Astrophysical turbulence modeling. *Rep. Prog. Phys.* **2011**, *74*, 046901. [CrossRef]
121. Mininni, P.D. Scale Interactions in Magnetohydrodynamic Turbulence. *Ann. Rev. Fluid Mech.* **2011**, *43*, 377. [CrossRef]
122. Brandenburg, A.; Sokoloff, D.; Subramanian, K. Current Status of Turbulent Dynamo Theory. *Space Sci. Rev.* **2012**, *169*, 123. [CrossRef]
123. Brandenburg, A.; Lazarian, A. Astrophysical Hydromagnetic Turbulence. *Space Sci. Rev.* **2013**, *178*, 163. [CrossRef]
124. Matthaeus, W.H.; Montgomery, D.C.; Wan, M.; Servidio, S. A review of relaxation and structure in some turbulent plasmas: Magnetohydrodynamics and related models. *J. Turbul.* **2013**, *13*, N37. [CrossRef]
125. Veltri, P. MHD turbulence in the solar wind: Self-similarity, intermittency and coherent structures. *Plasma Phys. Control. Fusion* **1999**, *41*, A787. [CrossRef]
126. Mininni, P.D.; Pouquet, A. Finite dissipation and intermittency in magnetohydrodynamics. *Phys. Rev. E* **2009**, *80*, 025401. [CrossRef] [PubMed]
127. Greco, A.; Matthaeus, W.H.; Servidio, S.; Chuychai, P.; Dmitruk, P. Statistical analysis of discontinuities in solar wind ACE data and comparison with intermittent MHD turbulence. *Astrophys. J.* **2009**, *691*, L111. [CrossRef]
128. Martin, L.N.; Vita, G.D.; Sorriso-Valvo, L.; Dmitruk, P.; Nigro, G.; Primavera, L.; Carbone, V. Cancellation properties in hall magnetohydrodynamics with a strong guide magnetic field. *Phys. Rev. E* **2013**, *88*, 063107. [CrossRef] [PubMed]
129. Zhdankin, V.; Uzdensky, D.A.; Perez, J.C.; Boldyrev, S. Statistical analysis of current sheets in three-dimensional magnetohydrodynamic turbulence. *Astrophys. J.* **2013**, *771*, 124. [CrossRef]
130. Zhdankin, V.; Boldyrev, S.; Perez, J.C.; Tobias, S.M. Energy dissipation in magnetohydrodynamic turbulence: Coherent structures or "nanoflares"? *Astrophys. J.* **2014**, *795*, 127. [CrossRef]
131. Parashar, T.N.; Matthaeus, W.H. Propinquity of current and vortex structures, effects on collisionless plasma heating. *Astrophys. J.* **2016**, *832*, 57. [CrossRef]
132. Kitiashvili, I.N.; Kosovichev, A.G.; Mansour, N.N.; Lele, S.K.; Wray, A.A. Vortex tubes of turbulent solar convection. *Phys. Scr.* **2012**, *86*, 018403. [CrossRef]
133. Kivotides, D. Interactions between vortex tubes and magnetic-flux rings at high kinetic and magnetic Reynolds numbers. *Phys. Rev. Fluids* **2018**, *3*, 033701. [CrossRef]
134. Silva, S.S.A.; Fedun, V.; Verth, G.; Rempel, E.L.; Shelyag, S. Solar Vortex Tubes: Vortex Dynamics in the Solar Atmosphere. *Astrophys. J.* **2020**, *898*, 137. [CrossRef]
135. Wan, M.; Oughton, S.; Servidio, S.; Matthaeus, W.H. Von Kármán self-preservation hypothesis for magnetohydrodynamic turbulence and its consequences for universality. *J. Fluid Mech.* **2012**, *697*, 296. [CrossRef]
136. Lee, E.; Brachet, M.E.; Pouquet, A.; Mininni, P.D.; Rosenberg, D. Lack of universality in decaying magnetohydrodynamic turbulence. *Phys. Rev. E* **2010**, *81*, 016318. [CrossRef] [PubMed]
137. Ohno, N.; Ohtani, H. Development of In-Situ Visualization Tool for PIC Simulation. *Plasma Fusion Res.* **2015**, *9*, 3401071. [CrossRef]
138. Stawarz, J.E.; Pouquet, A. Small-scale behavior of Hall magnetohydrodynamic turbulence. *Phys. Rev. E* **2015**, *92*, 063102. [CrossRef] [PubMed]
139. Banerjee, S.; Halder, A. Fundamental units of triadic interactions in Hall magnetohydrodynamic turbulence: How far can we go. *arXiv* **2023**, arXiv:2312.10709v1. [CrossRef]
140. Araki, K.; Miura, H. Asymmetry of Quadratic Energy Transfer Between Ion Cyclotron and whistler Modes in Fully Developed Hall Magnetohydrodynamic Turbulence. *Plasma Fusion Res.* **2020**, *15*, 2401024. [CrossRef]
141. Chong, M.S.; Perry, A.E.; Cantwell, B.J. A general classification of three-dimensional flow fields. *Phys. Fluids A* **1990**, *2*, 765. [CrossRef]
142. Yadav, S.K.; Miura, H.; Pandit, R. Statistical properties of three-dimensional Hall magnetohydrodynamics turbulence. *Phys. Fluids* **2022**, *34*, 095135. [CrossRef]
143. Ji, H.; Daughton, W.; Jara-Almonte, J.; Le, A.; Stanier, A.; Yoo, J. Magnetic reconnection in the era of exascale computing and multiscale experiments. *Nat. Rev. Phys.* **2022**, *4*, 263. [CrossRef]
144. Huba, J.D.; Rudakov, L.I. Hall Magnetic Reconnection Rate. *Phys. Rev. Lett.* **2004**, *93*, 175003. [CrossRef]
145. Ren, Y.; Yamada, M.; Gerhardt, S.; Ji, H.; Kulsrud, R.; Kuritsyn, A. Experimental Verification of the Hall Effect during Magnetic Reconnection in a Laboratory Plasma. *Phys. Rev. Lett.* **2005**, *95*, 055003. [CrossRef]
146. Eastwood, J.P.; Shay, M.A.; Phan, T.D.; Øieroset, M. Asymmetry of the Ion Diffusion Region Hall Electric and Magnetic Fields during Guide Field Reconnection: Observations and Comparison with Simulations. *Phys. Rev. Lett.* **2010**, *104*, 205001. [CrossRef] [PubMed]
147. Huang, Y.; Bhattacharjee, A.; Sullivan, B.P. Onset of fast reconnection in Hall magnetohydrodynamics mediated by the plasmoid instability. *Phys. Plasmas* **2011**, *18*, 072109. [CrossRef]

148. Lazarian, A.; Vlahos, L.; Kowal, G.; Yan, H.; Beresnyak, A.; Pino, E.M.d.D. Turbulence, Magnetic Reconnection in Turbulent Fluids and Energetic Particle Acceleration. *Space Sci. Rev.* **2012**, *173*, 557. [CrossRef]
149. Lazarian, A. Reconnection Diffusion in Turbulent Fluids and Its Implications for Star Formation. *Space Sci. Rev.* **2014**, *181*, 1. [CrossRef]
150. Osman, K.T.; Matthaeus, W.H.; Gosling, J.T.; Greco, A.; Servidio, S.; Hnat, B.; Chapman, S.C.; Phan, T.D. Magnetic reconnection and intermittent turbulence in the solar wind. *Phys. Rev. Lett.* **2014**, *112*, 215002. [CrossRef]
151. Lalescu, C.C.; Shi, Y.; Eyink, G.L.; Drivas, T.D. Inertial-Range Reconnection in Magnetohydrodynamic Turbulence and in the Solar Wind. *Phys. Rev. Lett.* **2015**, *115*, 025001. [CrossRef]
152. Boldyrev, S.; Loureiro, N. Magnetohydrodynamic Turbulence Mediated by Reconnection. *Astrophys. J.* **2017**, *844*, 125. [CrossRef]
153. Loureiro, N.F.; Boldyrev, S. Role of Magnetic Reconnection in Magnetohydrodynamic Turbulence. *Phys. Rev. Lett.* **2017**, *118*, 245101. [CrossRef]
154. Donato, S.; Servidio, S.; Dmitruk, P.; Carbone, V.; Shay, M.A.; Cassak, P.A.; Matthaeus, W.H. Reconnection events in two-dimensional Hall magnetohydrodynamic turbulence. *Phys. Plasmas* **2012**, *19*, 092307. [CrossRef]
155. Yoshimatsu, K.; Kondo, Y.; Schneider, K.; Okamoto, N.; Hagiwara, H.; Farge, M. Wavelet-based coherent vorticity sheet and current sheet extraction from three-dimensional homogeneous magnetohydrodynamic turbulence. *Phys. Plasmas* **2009**, *16*, 082306. [CrossRef]
156. Donato, S.; Greco, A.; Matthaeus, W.H.; Servidio, S.; Dmitruk, P. How to identify reconnecting current sheets in incompressible Hall MHD turbulence. *J. Geophys. Res. Space Phys.* **2013**, *118*, 4033. [CrossRef]
157. Kageyama, A.; Yamada, T. An approach to exascale visualization: Interactive viewing of in-situ visualization. *Comput. Phys. Commun.* **2014**, *185*, 79. [CrossRef]
158. O'Leary, P.; Ahrens, J.; Jourdain, S.; Wittenburg, S.; Rogers, D.H.; Petersen, M. Cinema image-based in situ analysis and visualization of MPAS-ocean simulations. *Parallel Comput.* **2016**, *55*, 43. [CrossRef]
159. Kageyama, A.; Sakamoto, N.; Miura, H.; Ohno, N. Interactive Viewing of In-situ Visualization of MHD Simulation. *Plasma Fusion Res.* **2020**, *15*, 1401065. [CrossRef]
160. Kobayashi, H. Large eddy simulation of magnetohydrodynamic turbulent channel flows with local subgrid-scale model based on coherent structures. *Phys. Fluids* **2006**, *18*, 045107. [CrossRef]
161. Hamba, F.; Tsuchiya, M. Cross-helicity dynamo effect in magnetohydrodynamic turbulent channel flow. *Phys. Plasmas* **2010**, *17*, 012301. [CrossRef]
162. Chernyshov, A.A.; Karelsky, K.V.; Petrosyan, A.S. Subgrid-scale modeling for the study of compressible magnetohydrodynamic turbulence in space plasmas. *Phys.-Uspekhi* **2014**, *57*, 421. [CrossRef]
163. Miesch, M.; Matthaeus, W.; Brandenburg, A.; Petrosyan, A.; Pouquet, A.; Cambon, C.; Jenko, F.; Uzdensky, D.; Stone, J.; Tobias, S.; et al. Large-Eddy Simulations of Magnetohydrodynamic Turbulence in Heliophysics and Astrophysics. *Space Sci. Rev.* **2015**, *97* 137. [CrossRef]
164. Miura, H.; Araki, K.; Hamba, F. Hall effects and sub-grid-scale modeling in magnetohydrodynamic turbulence simulations. *J. Comput. Phys.* **2016**, *316*, 385. [CrossRef]
165. Miura, H.; Hamba, F. Sub-grid-scale model for studying Hall effects on macroscopic aspects of magnetohydrodynamic turbulence. *J. Comput. Phys.* **2022**, *448*, 110692. [CrossRef]
166. Miura, H.; Hamba, F. Numerical Simulations of Hall MHD Turbulence with Magnetization. *Plasma Fusion Res.* **2023**, *18*, 2401022. [CrossRef]
167. Garnier, E.; Adams, N.; Sagaut, P. *Large Eddy Simulation for Compressible Flows*; Springer: Berlin/Heidelberg, Germany, 2009.